This is a peer-reviewed, accepted author manuscript of the following research article: Kim, D. K., Li, S., Lee, J. R., Poh, B. Y., Benson, S., & Cho, N-K. (2022). An empirical formula to assess ultimate strength of initially deflected plate: Part 1 = propose the general shape and application to longitudinal compression. Ocean Engineering, 252, [111151]. https://doi.org/10.1016/j.oceaneng.2022.111151

# *An empirical formula to access ultimate strength of initially deflected plate: Part I = Propose the general shape and application to longitudinal compression*

*Do Kyun Kim [a,b]*, Shen Li [c], Jia Rong Lee [d], Bee Yee Poh [d], Simon Benson [e] and Nak-Kyun Cho [f]**

[a] *Department of Naval Architecture and Ocean Engineering, College of Engineering, Seoul National University, Seoul, South Korea*

[b] *Research Institute of Marine Systems Engineering, Seoul National University, Seoul, Korea*

[c] *Department of Naval Architecture,Ocean and Marine Engineering, University of Strathclyde, Glasgow, United Kingdom*

[d] *Ocean and Ship Technology (OST) Research Group, Department of Civil and Environmental Engineering, Universiti Teknologi PETRONAS, Seri Iskandar, Perak, Malaysia*

[e] *Group of Marine Offshore and Subsea Technology (MOST), School of Engineering, Newcastle University, Newcastle upon Tyne, United Kingdom*

[f] *Department of Manufacturing Systems and Design Engineering, Seoul National University of Science and Technology (SeoulTech), Seoul, Korea*

## *Abstract*

*This study proposes a simplified empirical formulation to predict the ultimate strength of the initially deflected plate subjected to longitudinal compression. The empirical formulation's applicability and accuracy were verified by comparing the nonlinear finite element method (NLFEM). In total, 700 cases of initially deflected plate scenarios by assuming the buckling mode shape were adopted as the input data. For the simplification of the plate design process, a general shape of the empirical formula is proposed based on input data. A reliable technical solution is obtained with good agreements ($R^2$ = 0.98 to 0.99) compared to NLFEM. The advantage of the proposed outcome is documented by comparing the previous study. The obtained result could be beneficial for the structural design of the initially deflected plate in predicting its ultimate strength performance under longitudinal compression.*

**Corresponding authors: Do Kyun Kim (do.kim@snu.ac.kr) and Nak-Kyun Cho (nkcho@seoultech.ac.kr).*

***Keywords:*** *Ultimate limit state, initial deflection, longitudinal compression, buckling shape, ships and offshore structures.*

## *1 Introduction*

*Ships and ship-shaped offshore structures are exposed to severe environmental conditions during operation, which may apply various actions (or loadings) to the marine structures (Kim et al., 2019b). The vertical bending moment (VBM), which is measured for ensuring the global strength of ships and ship-shaped offshore structures in the design stage, is considered the most important activity among the applied loadings in preventing the hull girder collapse. The continued axial compression and tension caused by hogging- and sagging-VBMs are affecting the structural safety of local structural components such as plate (= unstiffened panel) and stiffened panels (Paik et al., 2009).*

*The Common Structural Rule (CSR) for oil tanker (IACS, 2006b) and bulk carrier (IACS, 2006a) has been released by the International Association of Classification Societies (IACS). These rules were released to provide a common guideline, which means that each classification societies' rules were considered pre-CSR. One of the purposes was to highlight the importance of the limit state design (LSD) concept rather than the working stress design (WSD) technique previously used. Recently, both rules were released by IACS (2020), known as a Harmonised Common Structural Rule (CSR-H).*

*The LSD, also known as load and resistance factor design (LRFD), refers to a design method used in structural engineering and design application. The ultimate limit state (ULS), accident limit state (ALS), fatigue limit state (FLS), and serviceability limit state (SLS) can be subsumed under the LSD category (Paik, 2018). Concerning LSD, several studies have recently been conducted by many research groups (Ao et al., 2020; Doan et al., 2020; Georgiadis and Samuelides, 2019; ISSC, 2018; Jagite et al., 2019; Kong et al., 2020; Lee et al., 2019; Lee and Paik, 2020; Li and Benson, 2019; Li et al., 2020; Li et al., 2021; Shi and Gao, 2020; Tatsumi and Fujikubo, 2020; Tatsumi et al., 2020; Zhang et al., 2020).*

*In particular, the ultimate strength performances of the stiffened panel and plate need to be ensured in preventing the local failure phenomenon (Paik et al., 2009). In this regard, the*

*plate element is targeted, and its ultimate strength performance is investigated by proposing the simplified empirical formulation in this study. This primary structural component, plate element, is subjected to various loadings such as axial and biaxial compression, shear, lateral pressure, and many others. Many studies have been conducted to investigate the technique in predicting the ultimate strength performance of plate structure (Guedes Soares, 1988; Jiang and Guedes Soares, 2012; Paik et al., 2012a; Pei et al., 2010a; 2010b; Sadovský et al., 2005; Saeidifar et al., 2010; Teixeira et al., 2013; Ueda and Yao, 1985; Underwood et al., 2012; Zhang and Khan, 2009).*

*In particular, Paik et al. (2008) conducted a series of benchmark studies on the methods for assessing the ultimate limit state based structural safety by taking NLFEM (ANSYS), Semi-analytical (DNV/PULS and ALPS/ULSAP), and existing design guidelines (Common Structural Rule, CSR by IACS). They have concluded that plate element is significantly affected by initial deflection shape, boundary condition and applied loading condition. The detailed NLFEM technique for assessing the ULS calculation of the plate structures was also studied by Paik and Seo (2009).*

*Nowadays, various types of user-friendly in-house software are used in the shipbuilding industry and classification societies to design ships and offshore structures by adopting semi-analytical methods or empirical formulations based on their accumulated technical background (IACS, 2020). Nevertheless, the full finite element method (FEM) or computational fluid dynamics (CFD) method, which require higher computational cost, is still recommended for the detailed structural design of ships and offshore structures (ISSC, 2012).*

*Several studies have been performed to develop empirical formulations in predicting ULS of the plate since 19 century (Carlsen, 1977; Cui and Mansour, 1998; Dwight and Moxham, 1969; Faulkner, 1975; Gerard, 1957; Hughes, 1983; Paik et al., 2004; Smith et al., 1988; Soreide and Czujko, 1983; Timoshenko, 1936; Ueda et al., 1975; von Kármán, 1924; Winter, 1940). Besides, empirical formulations and simplified practical techniques for stiffened panels have also been widely conducted by several researchers (Khedmati et al., 2010; Kim et al., 2017; 2019a; 2020d; Lin, 1985; Ozdemir et al., 2018; Paik, 2007; Paik and Thayamballi, 1997; Tanaka et al., 2014; Zhang and Khan, 2009). The details may be referred to review studies (Cui and Mansour, 1998; Kim et al., 2018b; Zhang, 2016) and ISSC reports (ISSC, 2009, 2012, 2015, 2018).*

*Recently, Kim et al. (2018c) proposed an empirical formulation to predict the ultimate strength of the initially deflected plate under longitudinal compression based on FE simulation results. The formulation shown in Appendix (Eq. A1) is based on the initial deflection index (IDI), which consists of four sub-coefficients ( $c_1$ - $c_4$ ). These sub-coefficients vary with the initial deflection coefficient ( $C_{ID}$ ), which is one of the issues to be resolved. An advanced form of the empirical formulation consisting of four (4) fixed sub-coefficients is proposed in this regard. In addition, its applicability in predicting accurate ultimate strength performance of initially deflected plate under longitudinal compression is investigated.*

## 2 Methodology

*Nowadays, the importance of the data and its processing technique for optimisation are highly recognised by many researchers from various fields. Significantly, the importance of data technology is stressed by giant IT companies. The importance of data processing technique and its application to ships and offshore structural design is highlighted in many studies by Kim et al. (2020a; 2020b; 2020c; 2019b). In this section, the procedure to propose an empirical formulation in predicting the ultimate strength of initially deflected plate subject longitudinal compression is addressed.*

### 2.1 Selection of reliable plate scenarios

*The plate's reliable data collection to be used for modelling input should conduct as a first step. In general, the distribution of the probability density function (PDF) with sampling technique is used to select reliable scenarios to be used as input for assessing the structural condition (Kim et al., 2018a; 2013; Mohd et al., 2014; Paik et al., 2012b; Wong and Kim, 2018; Youssef et al., 2016). The plate, considered as a primary structural component to construct ships and offshore structures, can be simply defined by material properties [i.e., material tensile test results or stress-strain curve including material yield strength ( $s_Y$ ), Elastic modulus ( $E$ ), and others], and geometric properties [i.e., length of the plate ( $a$ ), breadth of the plate ( $b$ ), the thickness of plate ( $t$ )] as shown in Figure 1.*

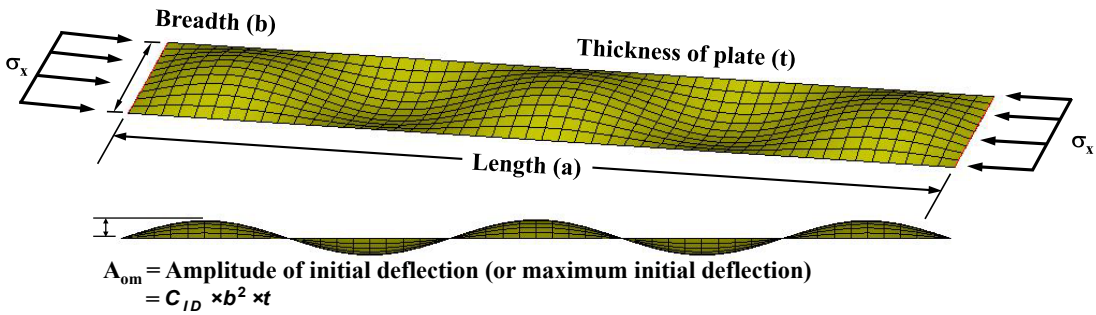


*Figure 1: Schematic view of the initially deflected plate (target structure).*

*Nowadays, data-driven prediction is one of the popular keywords in the world. In general, plate slenderness ratio ( $\boldsymbol{b}$ ) is used as a reference parameter by containing plate geometric properties ( $\boldsymbol{b}$, $\boldsymbol{t}$ ) and material properties ( $\boldsymbol{E}$ , $\boldsymbol{s_Y}$ ) as shown in Eq. (1).*

$$b = \frac{b}{t}\sqrt{\frac{s_Y}{E}} \qquad \text{Eq. (1)}$$

*To investigate the distribution of geometric and material properties of the plate element, recently, Kim et al. (2018c) collected the data from the twelve (12) representative commercial ships considering three (3) vessel types, i.e., oil tanker, bulk carrier, and container ship, with four (4) different sizes in each vessel type. They produced probability density functions (PDFs) in terms of plate's length, breadth, and thickness by conducting data processing, i.e., goodness-of-fit test, for collected plate data shown in Eqs. (2.1) to (2.3), respectively. It can also be referred to Fig. A.1.*

*From the Goodness-of-fit test results, they found that 3-Parameter Loglogistic function was suited in predicting the distribution of probability density of plate breadth, plate thickness, and plate slenderness ratio. In the case of the plate length, the logistic function was recommended. It was also obtained that the mean value of the geometric parameters of the plate (a, b, t) was a=4205.14mm, b= 837.07mm, and t = 18.30mm. The application of Goodness-of-fit test may be referred to (Kim et al., 2020b; Kim et al., 2020c).*

***Length of the plate (PDF: Logistic function)***

$$PDF = f(a) = \frac{\exp\left(\frac{a - B_1}{A_1}\right)}{A_1\left[1 + \exp\left(\frac{a - B_1}{A_1}\right)\right]^2} \qquad \text{Eq. (2.1)}$$

*where,* $\boldsymbol{a}$ *= length of plate,* $\boldsymbol{A_1}$ *= scale parameter (= 436.61), and* $\boldsymbol{B_1}$ *= location parameter (= 4205.14).*

***Breadth of the plate (PDF: 3-Parameter Loglogistic function)***

$$PDF = f(b) = \frac{\exp\left(\frac{\ln(b - C_2) - B_2}{A_2}\right)}{A_2(b - C_2)\left[1 + \exp\left(\frac{\ln(b - C_2) - B_2}{A_2}\right)\right]^2} \qquad \text{Eq. (2.2)}$$

*where,* $\boldsymbol{b}$ *= breadth of plate,* $\boldsymbol{A_2}$ *= scale parameter (= 0.06586),* $\boldsymbol{B_2}$ *= location parameter (= 6.9222) and* $\boldsymbol{C_2}$ *= threshold parameter (= -184.76).*

***Thickness of the plate (PDF: 3-Parameter Loglogistic function)***

$$PDF = f(t) = \frac{\exp\left(\frac{\ln(t - C_3) - B_3}{A_3}\right)}{A_3(t - C_3)\left[1 + \exp\left(\frac{\ln(t - C_3) - B_3}{A_3}\right)\right]^2} \qquad \text{Eq. (2.3)}$$

*where,* $\boldsymbol{t}$ *= breadth of plate,* $\boldsymbol{A_3}$ *= scale parameter (= 0.26893),* $\boldsymbol{B_3}$ *= location parameter (= 2.10671) and* $\boldsymbol{C_3}$ *= threshold parameter (= 9.00814).*

*In the material curve, a bilinear model type stress-strain curve with no tangential angle is adopted. The distribution of probability density (PD) of plate slenderness ratio (=* $\boldsymbol{b}$ *) was also investigated by Kim et al. (2018c), as shown in Eq. (2.4).*

***Plate slenderness ratio (PDF: 3-Parameter Loglogistic function)***

$$PDF = f(b) = \frac{\exp\left(\frac{\ln(b - C_4) - B_4}{A_4}\right)}{A_4(b - C_4)\left(1 + \exp\left(\frac{\ln(t - C_4) - B_4}{A_4}\right)\right)^2} \qquad \text{Eq. (2.4)}$$

*where,* $b$ *= breadth of plate,* $A_4$ *= scale parameter (= 0.0916),* $B_4$ *= location parameter (= 1.0132) and* $C_4$ *= threshold parameter (= -0.9026).*

*In fabrication, initial imperfections occur due to transportation, manufacturing, and many other reasons. In particular, the effects of initial distortion, initial deflection, welding-induced residual stress, initial crack, and initial dent are generally considered in the early design stage due to their uncertainties (Li et al., 2021). In the case of the plate, the following three (3) levels of initial deflection shown in Eq. (3.1) are suggested to be used as a guideline for structural analysis by Smith et al. (1988).*

*Initial deflection of the plate (*$w_{opl}$*) can be represented as a function of the coefficient of initial deflection (*$C_{ID}$*), plate slenderness ratio (*$b$*), and thickness of plate (*$t$*) as illustrated in Eq. (3.2). For in-depth investigation of initial deflection effect, additional four (4)* $C_{ID}$ *values were considered such as 0.05, 0.15, 0.20, and 0.25. To sum up, seven (7) levels of initial deflection of the plate are assumed to be added in plate scenarios.*

***Initial deflection amounts of plate proposed by Smith et al. (1988)***

$$w_{opl} = \begin{cases} 0.025b^2t & \text{for slight level} \\ 0.10b^2t & \text{for average level} \\ 0.30b^2t & \text{for severe level} \end{cases} \qquad \text{Eq. (3.1)}$$

***Initial deflection of the plate (General shape)***

$$w_{opl} = C_{ID}b^2t \qquad \text{Eq. (3.2)}$$

*where* $C_{ID}$ *= coefficient of initial deflection and the schematic view is shown in Figure 1.*

*Concerning the shape and amplitude of initial deflection, which is important parameters in this study, the buckling mode of deflection with the maximum amplitude is assumed. We are aware that Smith's provided the measured maximum initial deflection based on hungry horse mode, and it may be considered equivalent amplitude of initial deformation in a simple manner. The sinusoidal form of initial deflection with the amplitude of Smith's formula is unrealistic, and it may give an over-conservative estimate of the ultimate strength. However, the proposed empirical formula, which is going to be presented in Eq. (7.1) and (7.2), is the function of the initial deflection coefficient ($C_{ID}$), plate slenderness ratio ($b$), and the other four coefficients ($k_1$ to $k_4$). This $C_{ID}$ may enable us to consider the measured initial deflection amount. In addition, underrated ultimate strength by assuming buckling mode with maximum deflection may allow us to secure an additional safety margin.*

*From the above procedure with PDFs, 100 cases of plate scenarios are generated based on geometric and material properties, as shown in Eq. (4) and Table 1. In brief, fixed values of the length (a = 4150mm) and breadth (b = 830mm) of the plate are selected based on the achieved PDF, while a wide range of the thickness of the plate is considered by considering two (2) representative material yield strengths (235 and 315MPa) so that the effect of variation of plate slenderness ratio on ultimate strength performance of plate can be investigated. In the case of elastic modulus (E), the fixed value of 205.8GPa (= 205,800MPa) is assumed. With selected hundred (100) plate scenarios, seven (7) levels of initial deflection are considered. It means that seven hundred (700) plate scenarios are used for FE modelling input in total, and the FE results should be used for input data in developing the empirical formulation.*

$$\underbrace{\left(1 \times 1 \times 50\right)}_{\text{geometric}} \times \underbrace{\left(2 \times 1\right)}_{\text{material}} \times \underbrace{\left(7\right)}_{\text{initial deflection}} = 700^{\text{scenarios}} \qquad \text{Eq. (4)}$$

*Table 1: Selected plate scenarios (Kim et al., 2018c).*

| No | $a$ (mm) | $b$ (mm) | $t$ (mm) | $s_Y$ (MPa) | $E$ (GPa) | $b$ | $C_{ID}$ |
|---|---|---|---|---|---|---|---|
| 1 | 4150 | 830 | 44.50 | 315 | 205.8 | 0.73 | ***7 cases*** |
| 2 | 4150 | 830 | 38.50 | 315 | 205.8 | 0.84 | 0.025 |

| | | | | | | | |
|---|---|---|---|---|---|---|---|
| 3 | 4150 | 830 | 36.00 | 315 | 205.8 | 0.90 | 0.05 |
| 4 | 4150 | 830 | 34.00 | 315 | 205.8 | 0.96 | 0.10 |
| 5 | 4150 | 830 | 32.50 | 315 | 205.8 | 1.00 | 0.15 |
| 6 | 4150 | 830 | 31.50 | 315 | 205.8 | 1.03 | 0.20 |
| 7 | 4150 | 830 | 31.00 | 315 | 205.8 | 1.05 | 0.25 |
| 8 | 4150 | 830 | 30.00 | 315 | 205.8 | 1.08 | 0.30 |
| 9 | 4150 | 830 | 29.50 | 315 | 205.8 | 1.10 | |
| 10 | 4150 | 830 | 29.00 | 315 | 205.8 | 1.12 | |
| 11 | 4150 | 830 | 28.50 | 315 | 205.8 | 1.14 | |
| 12 | 4150 | 830 | 28.00 | 315 | 205.8 | 1.16 | |
| 13 | 4150 | 830 | 27.50 | 315 | 205.8 | 1.18 | |
| 14 | 4150 | 830 | 27.00 | 315 | 205.8 | 1.20 | |
| 15 | 4150 | 830 | 26.50 | 315 | 205.8 | 1.23 | |
| 16 | 4150 | 830 | 26.00 | 315 | 205.8 | 1.25 | |
| 17 | 4150 | 830 | 25.50 | 315 | 205.8 | 1.27 | |
| 18 | 4150 | 830 | 25.00 | 315 | 205.8 | 1.30 | |
| 19 | 4150 | 830 | 24.50 | 315 | 205.8 | 1.33 | |
| 20 | 4150 | 830 | 24.00 | 315 | 205.8 | 1.35 | |
| 21 | 4150 | 830 | 23.50 | 315 | 205.8 | 1.38 | |
| 22 | 4150 | 830 | 23.00 | 315 | 205.8 | 1.41 | |
| 23 | 4150 | 830 | 22.50 | 315 | 205.8 | 1.44 | |
| 24 | 4150 | 830 | 22.00 | 315 | 205.8 | 1.48 | |
| 25 | 4150 | 830 | 21.50 | 315 | 205.8 | 1.51 | |
| 26 | 4150 | 830 | 21.00 | 315 | 205.8 | 1.55 | |
| 27 | 4150 | 830 | 20.50 | 315 | 205.8 | 1.58 | |
| 28 | 4150 | 830 | 20.00 | 315 | 205.8 | 1.62 | |
| 29 | 4150 | 830 | 19.50 | 315 | 205.8 | 1.67 | |
| 30 | 4150 | 830 | 19.00 | 315 | 205.8 | 1.71 | |
| 31 | 4150 | 830 | 18.50 | 315 | 205.8 | 1.76 | |
| 32 | 4150 | 830 | 18.00 | 315 | 205.8 | 1.80 | |
| 33 | 4150 | 830 | 17.50 | 315 | 205.8 | 1.86 | |
| 34 | 4150 | 830 | 17.00 | 315 | 205.8 | 1.91 | |
| 35 | 4150 | 830 | 16.50 | 315 | 205.8 | 1.97 | |
| 36 | 4150 | 830 | 16.00 | 315 | 205.8 | 2.03 | |
| 37 | 4150 | 830 | 15.50 | 315 | 205.8 | 2.09 | |
| 38 | 4150 | 830 | 15.00 | 315 | 205.8 | 2.16 | |
| 39 | 4150 | 830 | 14.50 | 315 | 205.8 | 2.24 | |
| 40 | 4150 | 830 | 14.00 | 315 | 205.8 | 2.32 | |
| 41 | 4150 | 830 | 13.50 | 315 | 205.8 | 2.41 | |

| | | | | | | | |
|---|---|---|---|---|---|---|---|
| 42 | 4150 | 830 | 13.00 | 315 | 205.8 | 2.50 | |
| 43 | 4150 | 830 | 12.50 | 315 | 205.8 | 2.60 | |
| 44 | 4150 | 830 | 12.00 | 315 | 205.8 | 2.71 | |
| 45 | 4150 | 830 | 11.50 | 315 | 205.8 | 2.82 | |
| 46 | 4150 | 830 | 11.00 | 315 | 205.8 | 2.95 | |
| 47 | 4150 | 830 | 10.50 | 315 | 205.8 | 3.09 | |
| 48 | 4150 | 830 | 10.00 | 315 | 205.8 | 3.25 | |
| 49 | 4150 | 830 | 9.50 | 315 | 205.8 | 3.42 | |
| 50 | 4150 | 830 | 8.50 | 315 | 205.8 | 3.82 | |
| 51 | 4150 | 830 | 42.00 | 235 | 205.8 | 0.67 | |
| 52 | 4150 | 830 | 36.50 | 235 | 205.8 | 0.77 | |
| 53 | 4150 | 830 | 34.00 | 235 | 205.8 | 0.82 | |
| 54 | 4150 | 830 | 32.00 | 235 | 205.8 | 0.88 | |
| 55 | 4150 | 830 | 30.50 | 235 | 205.8 | 0.92 | |
| 56 | 4150 | 830 | 29.50 | 235 | 205.8 | 0.95 | |
| 57 | 4150 | 830 | 29.00 | 235 | 205.8 | 0.97 | |
| 58 | 4150 | 830 | 28.50 | 235 | 205.8 | 0.98 | |
| 59 | 4150 | 830 | 27.50 | 235 | 205.8 | 1.02 | |
| 60 | 4150 | 830 | 27.00 | 235 | 205.8 | 1.04 | |
| 61 | 4150 | 830 | 26.50 | 235 | 205.8 | 1.06 | |
| 62 | 4150 | 830 | 26.00 | 235 | 205.8 | 1.08 | |
| 63 | 4150 | 830 | 25.50 | 235 | 205.8 | 1.10 | |
| 64 | 4150 | 830 | 25.00 | 235 | 205.8 | 1.12 | |
| 65 | 4150 | 830 | 24.50 | 235 | 205.8 | 1.14 | |
| 66 | 4150 | 830 | 24.00 | 235 | 205.8 | 1.17 | |
| 67 | 4150 | 830 | 23.50 | 235 | 205.8 | 1.19 | |
| 68 | 4150 | 830 | 23.00 | 235 | 205.8 | 1.22 | |
| 69 | 4150 | 830 | 22.50 | 235 | 205.8 | 1.25 | |
| 70 | 4150 | 830 | 22.00 | 235 | 205.8 | 1.27 | |
| 71 | 4150 | 830 | 21.50 | 235 | 205.8 | 1.30 | |
| 72 | 4150 | 830 | 21.00 | 235 | 205.8 | 1.34 | |
| 73 | 4150 | 830 | 20.50 | 235 | 205.8 | 1.37 | |
| 74 | 4150 | 830 | 20.00 | 235 | 205.8 | 1.40 | |
| 75 | 4150 | 830 | 19.50 | 235 | 205.8 | 1.44 | |
| 76 | 4150 | 830 | 19.00 | 235 | 205.8 | 1.48 | |
| 77 | 4150 | 830 | 18.50 | 235 | 205.8 | 1.52 | |
| 78 | 4150 | 830 | 18.00 | 235 | 205.8 | 1.56 | |
| 79 | 4150 | 830 | 17.50 | 235 | 205.8 | 1.60 | |
| 80 | 4150 | 830 | 17.00 | 235 | 205.8 | 1.65 | |

| | | | | | | | |
|---|---|---|---|---|---|---|---|
| 81 | 4150 | 830 | 16.50 | 235 | 205.8 | 1.70 | |
| 82 | 4150 | 830 | 16.00 | 235 | 205.8 | 1.75 | |
| 83 | 4150 | 830 | 15.50 | 235 | 205.8 | 1.81 | |
| 84 | 4150 | 830 | 15.00 | 235 | 205.8 | 1.87 | |
| 85 | 4150 | 830 | 14.50 | 235 | 205.8 | 1.93 | |
| 86 | 4150 | 830 | 14.00 | 235 | 205.8 | 2.00 | |
| 87 | 4150 | 830 | 13.50 | 235 | 205.8 | 2.08 | |
| 88 | 4150 | 830 | 13.00 | 235 | 205.8 | 2.16 | |
| 89 | 4150 | 830 | 12.50 | 235 | 205.8 | 2.24 | |
| 90 | 4150 | 830 | 12.00 | 235 | 205.8 | 2.34 | |
| 91 | 4150 | 830 | 11.50 | 235 | 205.8 | 2.44 | |
| 92 | 4150 | 830 | 11.00 | 235 | 205.8 | 2.55 | |
| 93 | 4150 | 830 | 10.50 | 235 | 205.8 | 2.67 | |
| 94 | 4150 | 830 | 10.00 | 235 | 205.8 | 2.80 | |
| 95 | 4150 | 830 | 9.50 | 235 | 205.8 | 2.95 | |
| 96 | 4150 | 830 | 9.00 | 235 | 205.8 | 3.12 | |
| 97 | 4150 | 830 | 8.50 | 235 | 205.8 | 3.30 | |
| 98 | 4150 | 830 | 8.00 | 235 | 205.8 | 3.51 | |
| 99 | 4150 | 830 | 7.50 | 235 | 205.8 | 3.74 | |
| 100 | 4150 | 830 | 7.00 | 235 | 205.8 | 4.01 | |

## 2.2 *Structural modelling and analysis*

*The numerical method has become popular and widely used in various fields, i.e., engineering, science, and many others, along with its high effectiveness. An essential prerequisite for accurate results is that proper modelling techniques and appropriate scenario selections are essential. Many studies have been conducted in this connection, especially on the structural modelling techniques, which are still in great interest these days (ISSC, 2012).*

*The International Ship and offshore Structures Congress (ISSC) is one of the well-known congresses that provides valuable information through their research outcomes produced by the expert group (so-called ISSC report). The scope of the ISSC includes transportation, exploration, and exploitation of resources in and under the ocean by ships and ocean/marine structures. Remarkably, one of the technical committees (III.1 Ultimate strength) produced a wide range of investigation reports in terms of FE modelling technique, analysis method, and its verification*

*studies for the ultimate strength of ships and ocean/marine structures (ISSC, 2009, 2012, 2015, 2018).*

*In the present study, the ultimate strength outcomes computed by ANSYS NLFEM are considered input data in developing the empirical formulation. Details on the procedure for input data generations such as the selection of plate scenarios, structural modelling (i.e., geometry and material modelling, boundary condition, applied loading type, and others) and structural analysis are documented in this section.*

*As would be expected, the plate edge boundary condition in a continuous stiffened panel or plate structure is neither simply supported nor clamped. The torsional rigidity causes this at the plate edges, which is neither zero nor infinite, of the support members such as stiffener, transverse frame, longitudinal girder, and others (Paik et al., 2012a). It is well recognised that the effect of the plate edge condition may significantly affect the post-buckling behaviour of the plate element. In general, a simply supported (SS) boundary condition employs in predicting ULS behaviour while the actual condition is in between simply supported and clamped (CL) conditions. This SS condition may help to underrate the plate's actual ULS by allowing the maximum deflection, which means an additional safety margin may effectively be secured by adopting a pessimistic prediction option. On the other hand, we can reduce the uncertainty of the structural strength capacity by assuming the SS boundary condition, which can also be considered the worst condition.*

*Furthermore, it is required that a clear definition of the extent of plate modelling size should be confirmed so that reliable simulation results can be achieved. In general, one-bay & one-span (1-1) or two-bay & two-span or three-bay & three-span modelling technique is recommended for the finite element (FE) modelling of the plate (Paik, 2018; Paik and Thayamballi, 2007). In the present study, one bay & one span plate model is selected for FE analysis based on ISSC (2012). In the case of longitudinal girders and transverse frames, those are replaced by boundary conditions in this study. Longitudinal compression only applies to the plate elements by adopting displacement control in ANSYS NLFEM. Details on the FE modelling technique may be referred to as ISSC (2012) and (Kim et al., 2018c), as shown in Fig. 2(a) and (b). The obtained ultimate limit state (ULS or ultimate strength capacity) will be utilised to develop the empirical formulation.*

*Finally, ten elements are allocated between stiffeners, meaning that deflected plate shape can represent well by dividing the relevant number of the elements.*

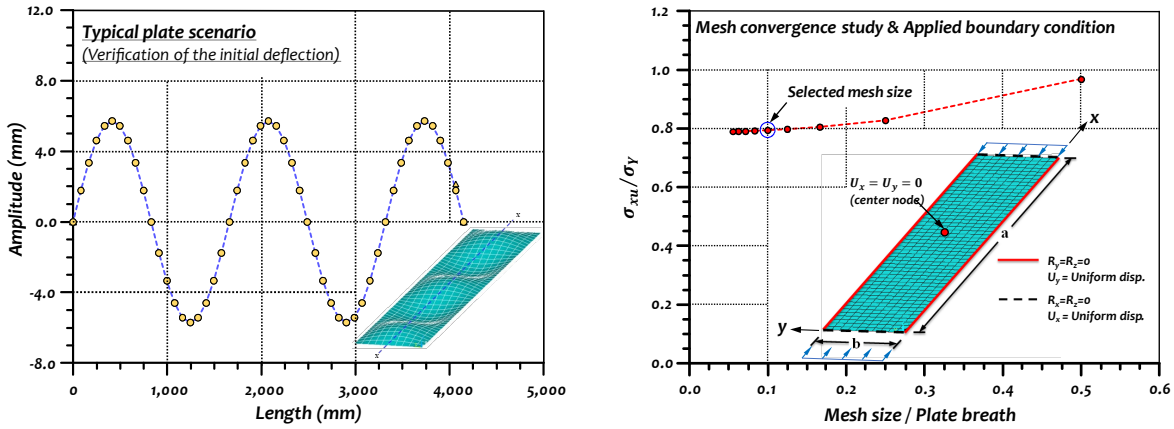


*(a) Initial deflection* *(b) boundary condition & mesh size*

*Figure 2: Typical example of FE modelling technique (Kim et al., 2018c)*

## 2.3 Analysis results & discussions

*Two groups of the results are presented in Figures 3 and 4 to investigate the effects of initial deflection and material yield strength on the plate's ultimate compressive strength, respectively. Figure 3(a) shows the behaviour of the plate's ultimate strength under longitudinal compression (= defined as ULS in the present study) as plate slenderness ratio increased. The ULS results of 700 scenarios are plotted considering seven different initial deflection levels in Figure 3(a). As expected, the ULS tends to decrease when the plate slenderness ratio increases or when the plate thickness is getting thinner. It is observed that ULS decreases faster when the level of the plate's initial deflection is severe. From the results observed in Figure 3(a), we investigated the effect of initial deflection in Figure 3(b) by calculating the mean and coefficient of variation (COV). As proposed by Smith et al. (1988), $C_{ID}$ = 0.1 represents the average level of the plate's initial deflection. For the comparison purpose in Figures 3(b) and 3(c), normalised Mean and COV were calculated based on the average level of the plate's initial deflection, which is widely used as a standard deflection amount for the plate analysis, in general.*

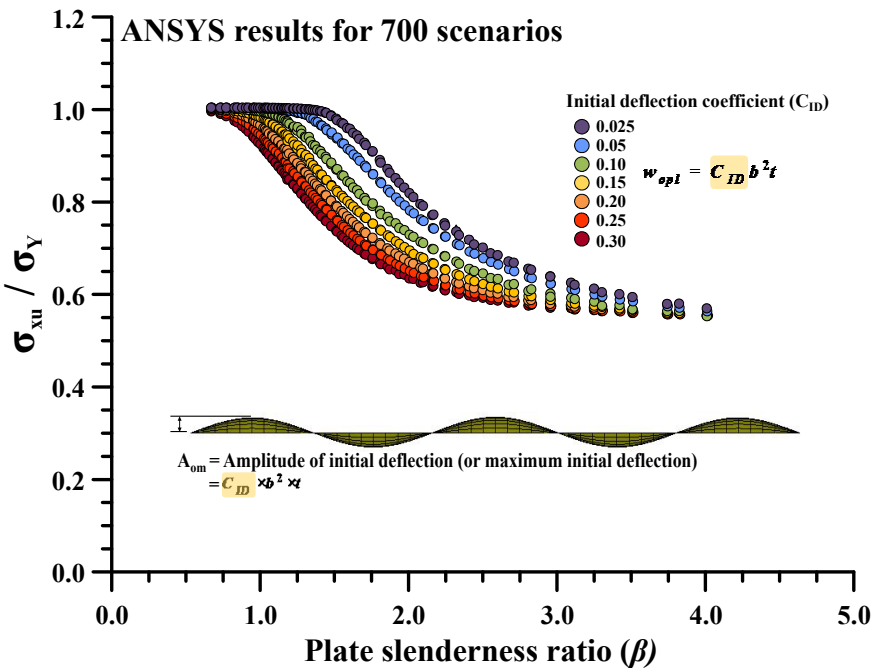


*(a) The obtained ULS results based on initial deflection coefficient*

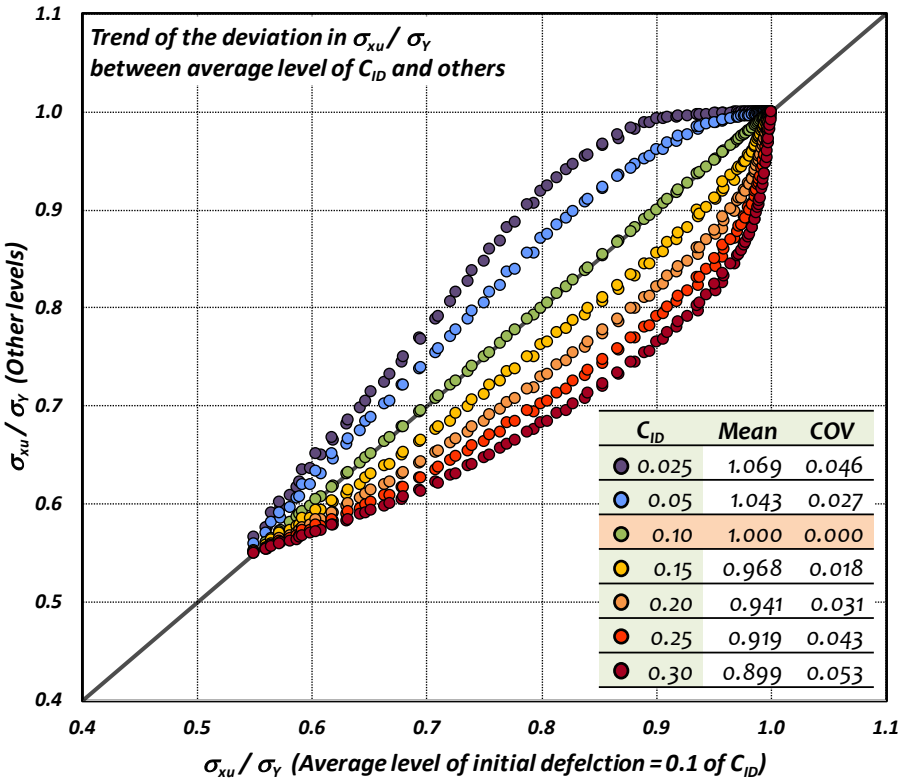


| $C_{ID}$ | Mean | COV |
|---|---|---|
| 0.025 | 1.069 | 0.046 |
| 0.05 | 1.043 | 0.027 |
| 0.10 | 1.000 | 0.000 |
| 0.15 | 0.968 | 0.018 |
| 0.20 | 0.941 | 0.031 |
| 0.25 | 0.919 | 0.043 |
| 0.30 | 0.899 | 0.053 |

*(b) Statistical analysis*

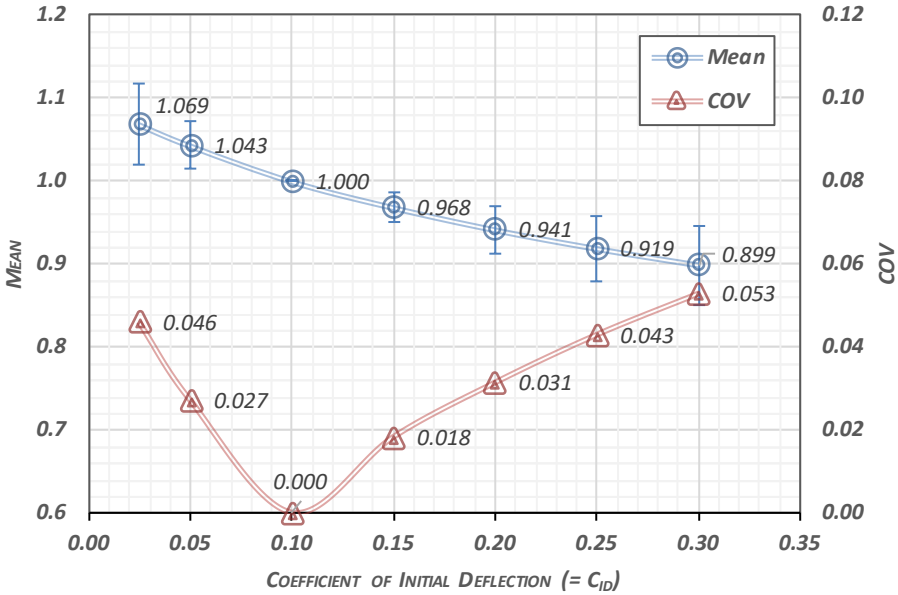


*(c) Mean and COV results*

*Figure 3: The ultimate strength behaviour of plate under longitudinal compression by considering initial deflection.*

*From the calculated mean value in Figure 3(c), a comparative analysis was performed based on the average level of plate deflection ($C_{ID}$ = 0.1), which is usually adopted in the shipyards and classification societies. We observed that the effect of initial deflection on the ULS from the slight level ($C_{ID}$ = 0.025) to the severe level ($C_{ID}$ = 0.3) was in the range between +6.9% to -10.1%. In general, initial imperfections are known to exist inevitably, among which initial deflection and welding-induced residual stress are considered. In particular, it can be understood that the range of the plate's initial deflection caused by the welding environment, i.e., welding condition, welder's proficiency, many others, has an effect of around 10% on ULS compared to the mean value shown in Fig. 3. In addition, the effect of the compressive residual stress on the ultimate strength of the stiffened panel is about 10-13% reported by Khan and Zhang (2011). The difference between slight and severe levels of initial plate deflection causes a 17% reduction of ULS.*

*We investigated a more precise difference for the research purpose by proposing the empirical formula shown in Eq. (5), which allows us to estimate the mean value due to the change of initial deflection coefficient ($C_{ID}$). At this point, we should remind that the initial deflection applied in this study is the buckling mode shape considered the idealised case. Also, the initial deflection features in the majority of plates show asymmetric and geometrically nonlinear characteristics*

*based on given boundary condition and related environmental condition, i.e., hungry horse, spoon, mountain and sinusoidal modes, as noted in many studies (Kim et al., 2012a; Paik et al., 2012a).*

$$Mean = 1.221C_{ID}^{2} - 1.001C_{ID} + 1.091 \quad (R^2 = 0.999) \qquad \text{Eq. (5)}$$

*Where,* $C_{ID}$ *= Coefficient of initial deflection, and* $R^2$ *= Coefficient of determination.*

*The effect of material yield strength is also followed by Figures 4(a) and (b). In this study, two materials such as mild steel (MS 24) and high tensile steel (HT32) with yield strength (i.e., 235 MPa and 315 MPa, respectively), are considered for the FE analysis. As observed in Figure 4(a), the effect of material yield strength does not significantly affect ULS behaviour. Statistical analysis was conducted in Figure 4(b) to investigate the effect of material yield strength on the ultimate strength performance of the plate in longitudinal compression. The empirical formulation by Kim et al. (2018c) is set as reference data. The mean (= 1.00 for HT32 and 1.01 for MS24) and COV values (= 0.008 for HT32; 0.110 for MS24) were obtained for each material in Figure 4(b). From this point of view, by adopting MS24 and HT32, we may carefully conclude that the effect of material yield strength on ULS changes may be negligible for the initially deflected flat plate. However, we should further investigate the effect of material yield strength on the ULS when the extra high strength steel, e.g., 690MPa or even higher yield strength.*

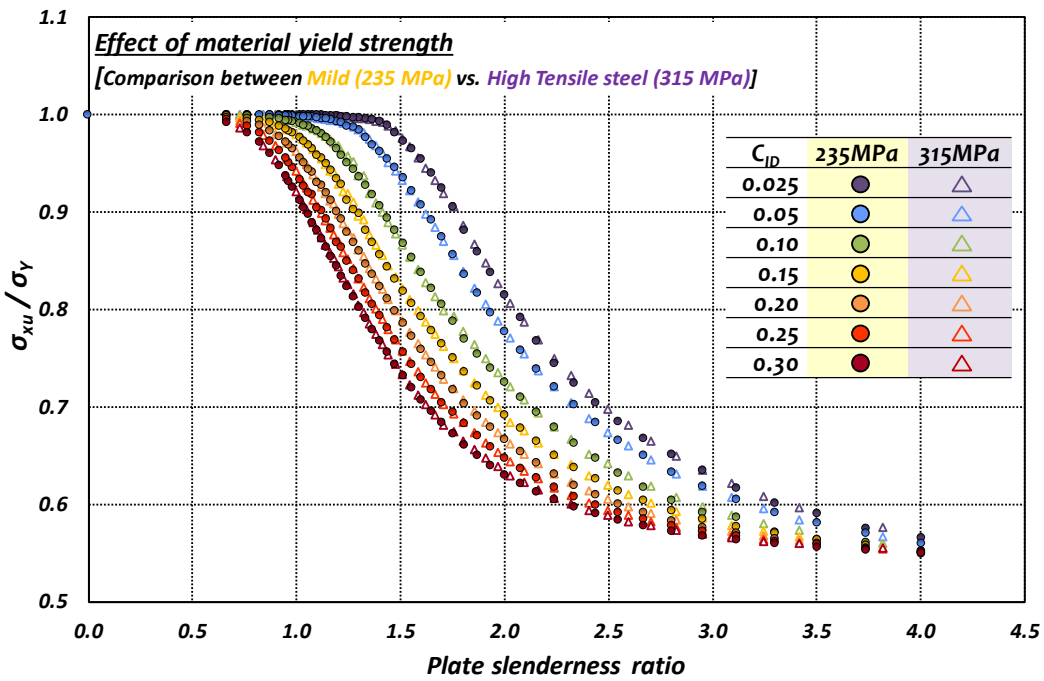


(a) The obtained ULS results based on material yield strength

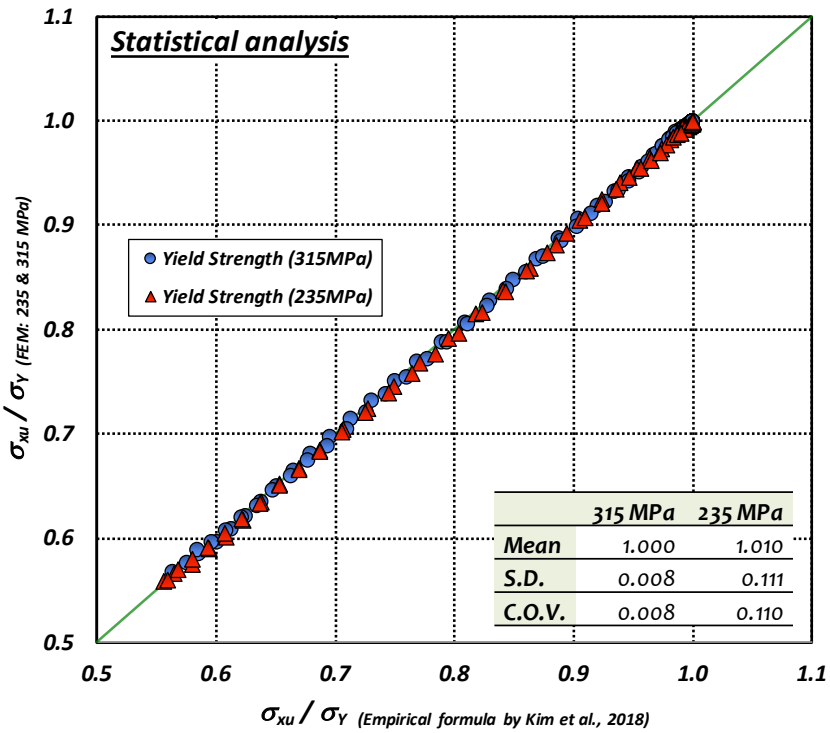


(b) Statistical analysis

Figure 4: The ultimate strength behaviour of plate under longitudinal compression by considering material yield strength.

*For a better understanding of the ULS behaviour of the plate, the von-Mises stress distributions at typical slenderness ratios ( **b** = near to 1.0, 2.0, 3.0, and 4.0) are further investigated in Figure 5. To observe Von-Mises stress distribution and deformed shape of the plate at ULS, the scale factors, i.e., 50 times, 20 times and five times respectively, are applied to individual plate slenderness ratios ( **b** =1.0, 2.0, 3.0 and 4.0). We found that different levels of initial deflections (i.e., $C_{ID}$ = 0.025, 0.05, 0.1, 0.15, 0.2, 0.25 and 0.3) was not affecting the pattern of deformation shape, which means that initially assumed buckling shape deformation was maintained at ULS. The importance of the assumed initial deflection shape can be recognised again. Furthermore, additional energy may require meaning that ULS is going to increase if the deformation pattern is changed as loading increased. We also reconfirm that the ULS of highly deflected plates (= higher $C_{ID}$) tend to decrease easier than slightly deflected plates (= lower $C_{ID}$).*

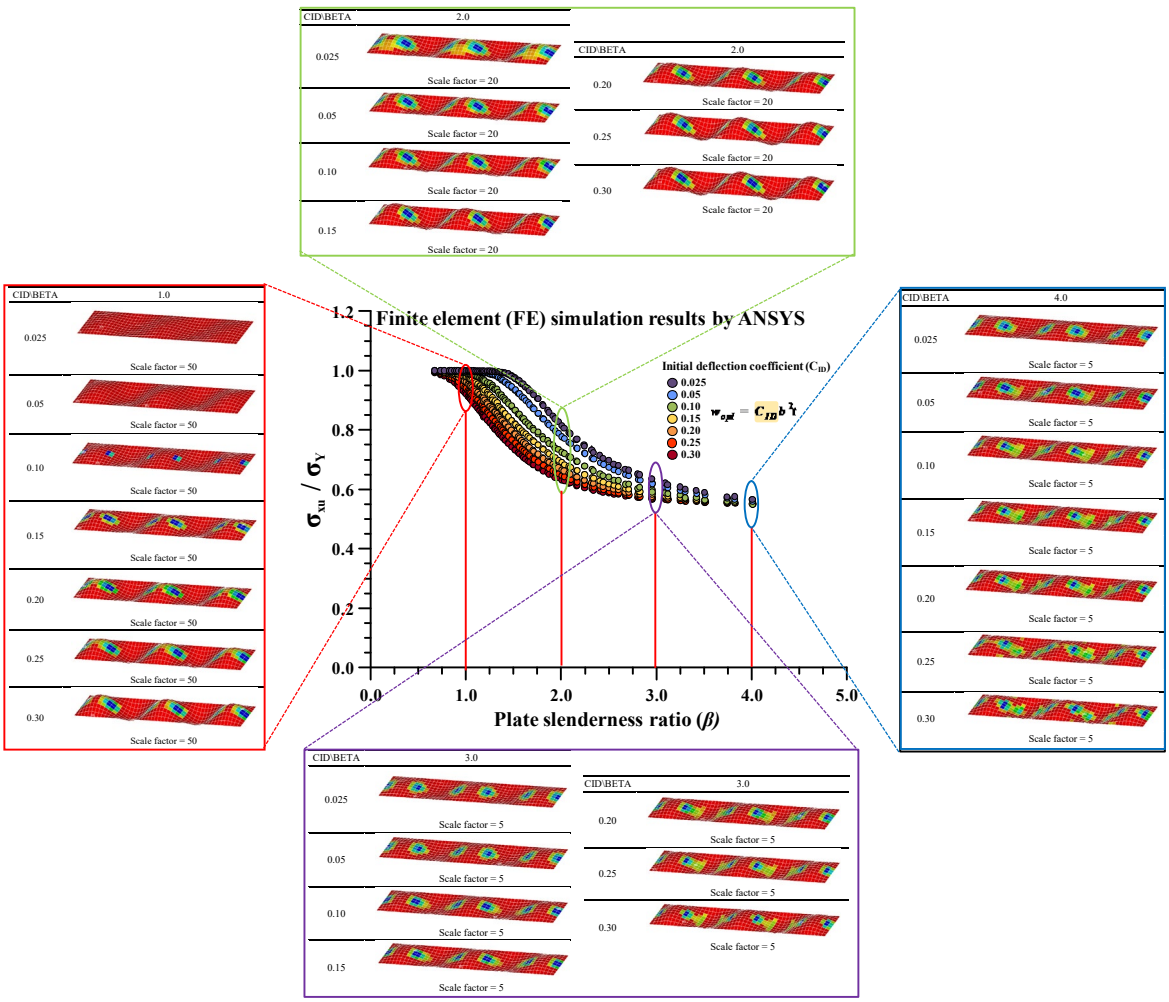


*Figure 5: Typical FE simulation results by von-Mises stress view.*

## 3 Development of general shape of empirical formulation

*The FE analysis results of 700 plate scenarios by Kim et al. (2018c) were utilised in developing the empirical formulation. The accuracy of the developed outcome was also verified by statistical analysis. The relationship between ULS by ANSYS NLFEM and plate slenderness ratio are presented in Figs. 6(a) to (g) to investigate the ULS behaviour of plate based on seven coefficients of initial defection ($C_{ID}$ = 0.025, 0.05, 0.10, 0.15, 0.20, 0.25 and 0.30). This means that each figure in Fig. 6 includes 100 cases of plate scenarios. The detailed scenarios may be referred to in Table 1.*

*As reviewed in the introduction part, various existing empirical formulations have been proposed based on the concept of effective width. In brief, the effective width concept is proposed to treat the redistribution of stresses by finding the edge stress along with the effectively contributing width of the plate shown in Eq. (6.1). This equation presents that true stresses can be replaced by two (2) uniform zones nearby edge parts, where the total zone width is $b_e$. Details may be referred to Paik (2008) or many other structural mechanics handbooks and lecture materials (Faulkner, 1975; von Kármán, 1924).*

$$\frac{b_e}{b} = \frac{s_{ave}}{s_e} \qquad \text{Eq. (6.1)}$$

*where, $b_e$ = effective breadth, $b$ = plate breadth, $s_{ave}$ = average post-buckling stress, $s_e$ = true edge stress which is the stress in $b_e$.*

*From this, many design and empirical formulations have been proposed as a shape of Eq. (6.2). We are aware that the ULS of the plate can be formulated as a function of the plate slenderness ratio, in general. Some researchers considered the effect of initial imperfections such as initial deflection, residual stress, and many other conditions. In this study, we proposed an empirical formulation based on plate slenderness ratio and initial deflection coefficient shown in Eq. (6.3). Several shapes of the plate's initial deflection include hungry horse, mountain, spoon, sinusoidal, and buckling mode (Kim et al., 2012b; Paik, 2018; Paik et al., 2004). Among others, the buckling shape of the initially deflected plate is solely considered in this study. Further studies may be recommended in developing the empirical formulations by adopting other types of initial deflection shapes.*

$$\frac{b_e}{b} = \frac{s_{xu}}{s_Y} \qquad \text{Eq. (6.2)}$$

$$\frac{s_{xu}}{s_Y} = f(b, C_{ID}, etc.) \qquad \text{Eq. (6.3)}$$

*where,* $s_{xu}$ *= ultimate compressive strength in x-axis (= ultimate longitudinal compressive strength, which is considered as ultimate strength in the present study),* $s_Y$ *= material yield strength,* $b$ *= plate slenderness ratio, and* $C_{ID}$ *= initial deflection coefficient, which can be referred to Eqs. (3.1) and (3.2).*

*The general shape of the empirical formulation proposed in this study is expressed in Eq. (7.1) as a function of two critical parameters, including the initial deflection coefficient and plate slenderness ratio. However, it could be extended to consider additional conditions such as other loadings, initial imperfections, boundary conditions, etc.*

*In Eq. (7.1) by this study, four coefficients, i.e.,* $k_1$, $k_2$, $k_3$ *and* $k_4$ *are introduced. These coefficients can be determined by the curve-fitting method. Moreover, different boundary conditions, loading conditions, and others may also be considered by formulating these four coefficients' sub-functions. In this study, we proposed empirical formulation by limiting the following conditions.*

- *Boundary condition: Simply supported plate*
- *Loading condition: Longitudinal compression*
- *Initial imperfection: Initial deflection only by assuming buckling mode shape*
- *Input data: numerical simulation results*

*The expected outcome by empirical formulation is the ultimate strength of the initially deflected plate subjected to longitudinal compression. The dimensionless result is provided by dividing ultimate strength (=* $s_{xu}$ *: ultimate compressive strength of plate in the longitudinal direction) to the material yield strength (* $s_Y$ *) as presented in the left-hand side of the Eq. (7.1). In*

*this study, the bi-linear shape material stress-strain curve is adopted without tangential slope. Therefore the ULS is assumed when structural strength reaches material yield. In other words,* $\sigma_{xu}/\sigma_Y$ *cannot exceed 1.0.*

***<u>Proposed empirical formulation shape (General)</u>***

$$\frac{\sigma_{xu}}{\sigma_Y} = 1 - \left[ k_1 \tan^{-1}\left( C_{ID} \times (b - C_{ID}) \times e^{k_2 \left( k_3 \times b + \frac{1}{C_{ID}^{k_4}} \right)^2} \right) \right]^6 \qquad \text{Eq. (7.1)}$$

*Where,* $b$ *= plate slenderness ratio,* $C_{ID}$ *= coefficient of initial deflection (of the plate),* $k_1, k_2$*,* $k_3$ *and* $k_4$ *= coefficients which can be determined based on assumed conditions.*

***<u>The empirical formulation</u>*** *<u>in predicting ULS of the initially deflected plate under longitudinal compression</u>*

$$\frac{\sigma_{xu}}{\sigma_Y} = 1 - \left[ 0.5552 \tan^{-1}\left( C_{ID} \times (b - C_{ID}) \times e^{1.2170 \left( 0.3193 b + \frac{1}{C_{ID}^{0.0605}} \right)^2} \right) \right]^6 \qquad \text{Eq. (7.2)}$$

*Note: Assumed conditions*

- *Boundary condition = Simply supported four edges;*
- *Initial deflection = buckling mode shape;*
- *Data = ULS data obtained by NLFEM;*
- *Loading type = Longitudinal compression only*

*The proposed Eq. (7.2) is achieved from the curve-fitting in Fig. 6(a) to (g) by determining the four coefficients (*$k_1$ *= 0.5552,* $k_2$ *= 1.2170,* $k_3$ *= 0.3193 and* $k_4$ *= 0.0605) in predicting ULS of plate under longitudinal compression based on assumed condition elaborated above. As proved in Fig. 6(a) to (g), the proposed empirical formulation in Eq. (7.2) shows good agreements (*$R^2$ *= 0.986 ~*

*0.990) with numerical simulation results by ANSYS nonlinear finite element method (NLFEM). We also observed that the ULS tends to decrease smoothly as plate slenderness ratio ( **b** ) increases. This trend and ULS values can be precisely predicted by the empirical formulation proposed in the present study.*

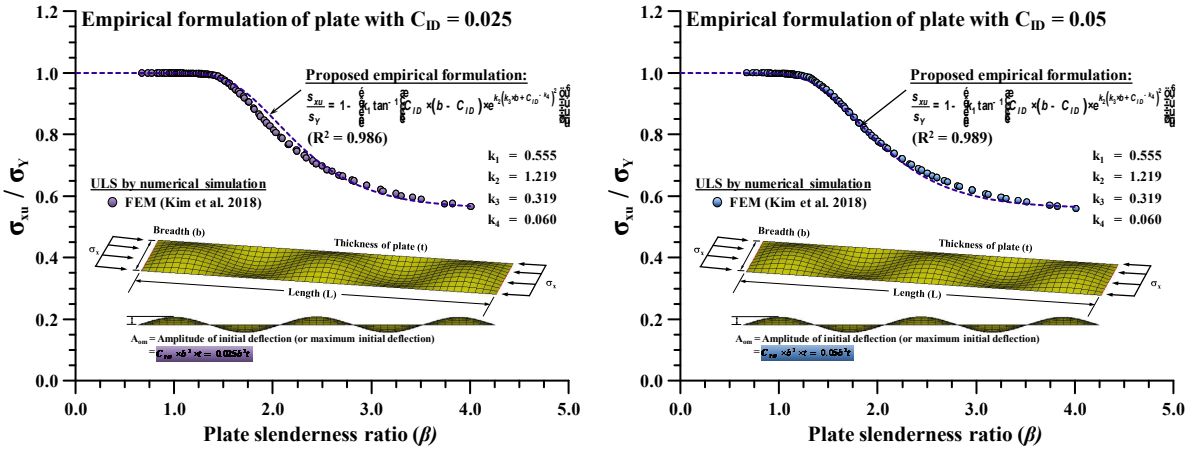


(a) $C_{ID}$ = 0.025 (Slight level)




(b) $C_{ID}$ = 0.05

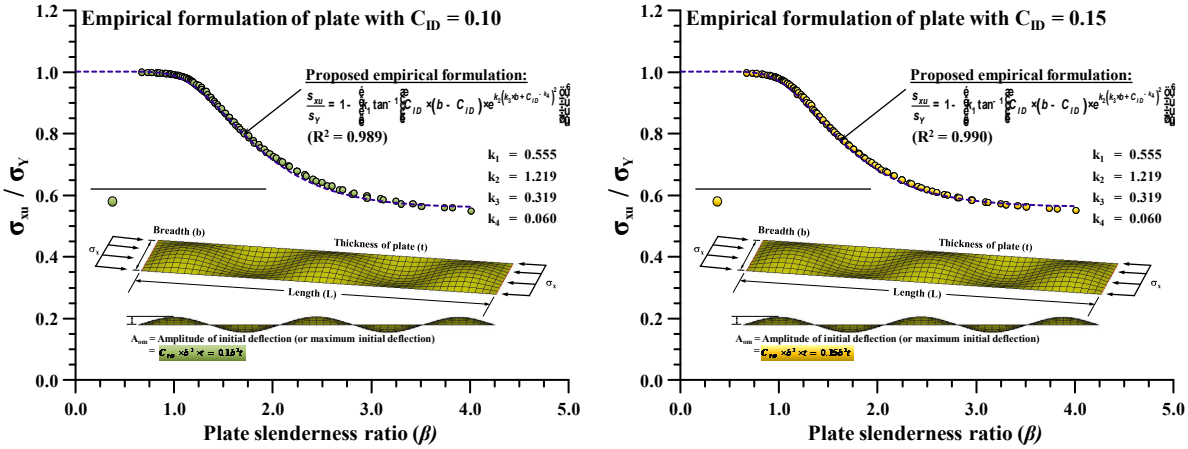


(c) $C_{ID}$ = 0.10 (= Average level)




(d) $C_{ID}$ = 0.15

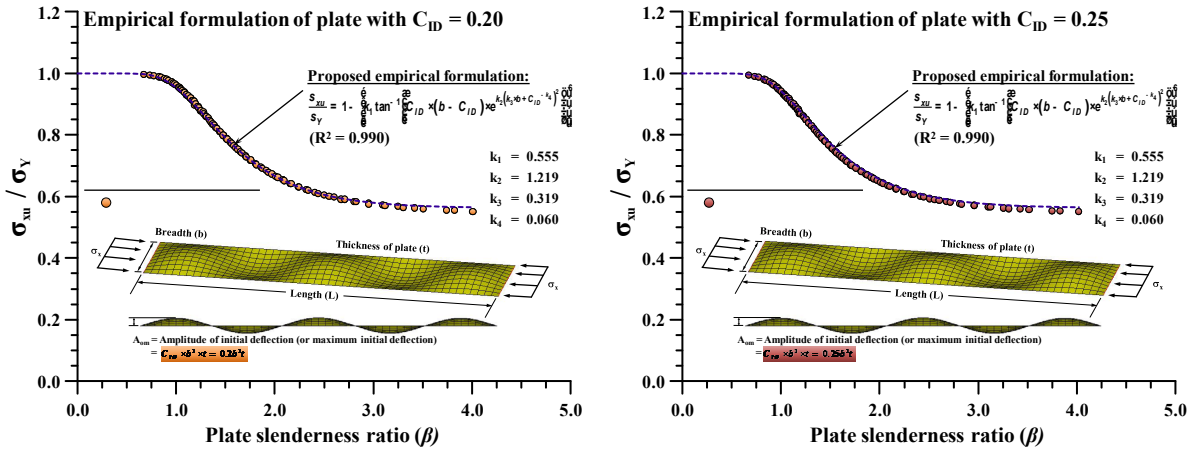


(e) $C_{ID}$ = 0.20 (f) $C_{ID}$ = 0.25

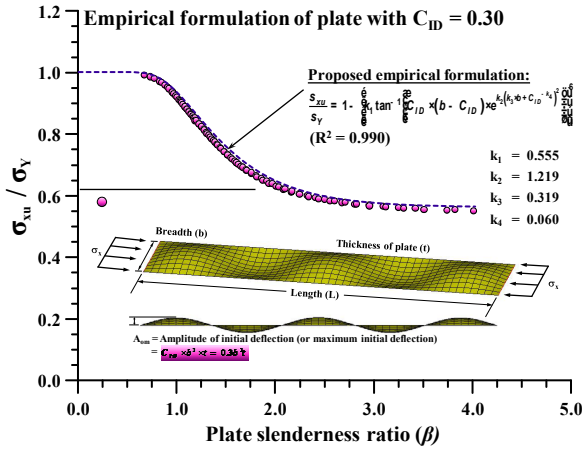


(g) $C_{ID}$ = 0.30 (= Severe level)

*Figure 6: Proposed empirical formulation and its accuracy by comparing with FEM initial (Note: $C_{ID}$ = Initial deflection coefficient).*

*To be more specific, the empirical formulation obtained by the curve-fitting method was well suited ($R^2$ ; 0.99) to the NLFEM when the initial deflection of the plate is large ($C_{ID}$ > 0.025). Simultaneously, the accuracy is slightly reduced ($R^2$ = 0.986) when the initial deflection is relatively tiny ($C_{ID}$ £ 0.025). The additional advantage of the empirical formulation proposed in this study goes to the four coefficients ($k_1$ to $k_4$), which are the constant values so that computational cost can be efficiently saved in predicting the ULS of plates. In contrast, the previous empirical formulation by Kim et al. (2018c) should conduct additional calculation of coefficients ($c_1$ to $c_4$) according to the changes of the $C_{ID}$.*

## 4 Discussions

*In line with the calculated* $R^2$ *values in Figs. 6(a) to (g), the accuracy of the empirical formulation proposed by the present study was validated by statistical analysis in Fig. 7(a). It is recognised that the good agreement between vertical (NLFEM) and horizontal (proposed formulation) axes can be present when the mean and COV values are closed to 1.0 and 0.0, respectively. Based on computed mean and COV values, we confirm the applicability of the empirical formulation proposed in predicting the ultimate strength of the plate under longitudinal compression. Furthermore, the empirical formulation's applicability may also be assessed whether it overestimates or underestimates the ultimate strength of the initially deflected plate from the mean value calculated. When the mean value exceeds 1.0, it represents the vertical axis results (= proposed empirical formulation) overestimates than the horizontal axis results (= NLFEM) while less than 1.0 shows underestimation. In this study, we assumed that the ULS results by NLFEM are set as a reliable outcome than the others.*

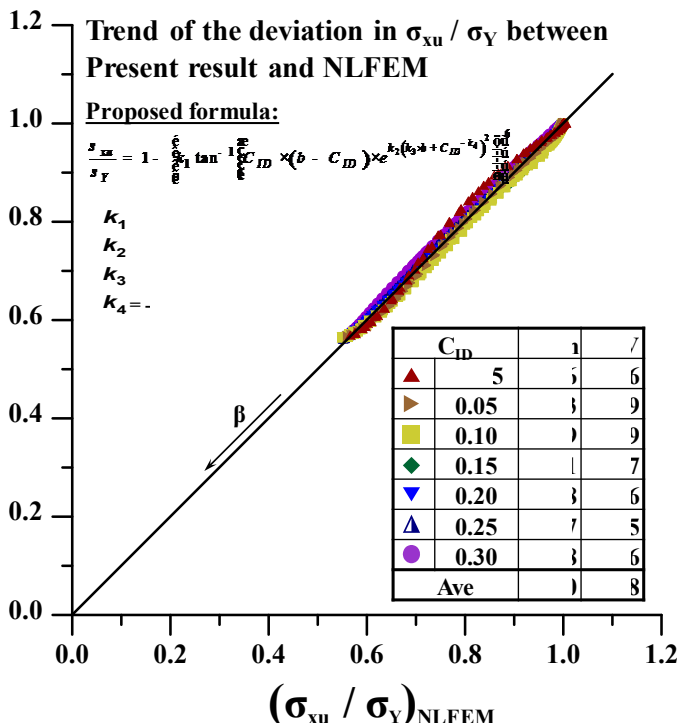


*(a) Mean and COV*

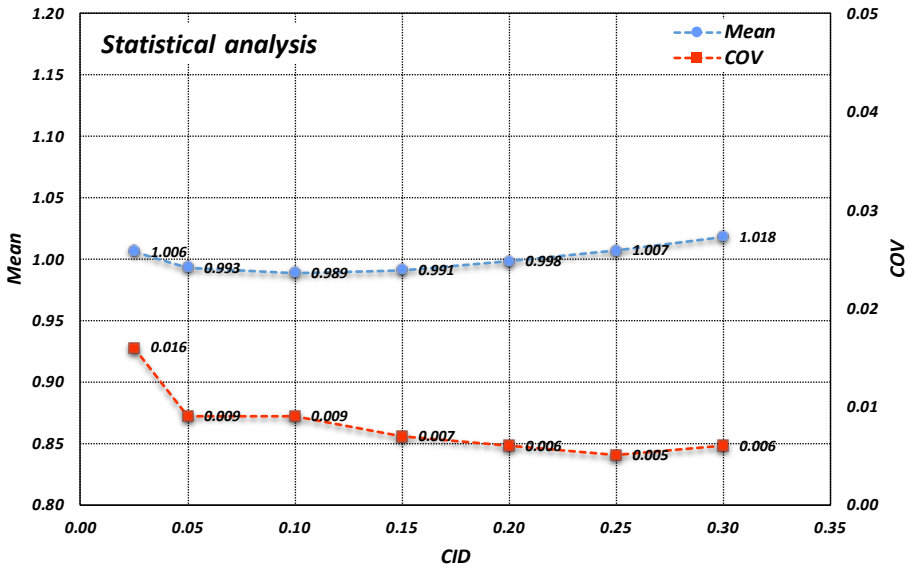


*(b) Based on the initial deflection coefficient*

*Figure 7: Statistical analysis results between FEM versus empirical formulation.*

*In general, the empirical formulation shows good agreement with NLFEM results from the average mean (= 1.000) and COV (= 0.008) values presented in Fig. 7(a). The changes of mean and COV values are also plotted based on adopted various initial deflection levels (i.e., $C_{ID}$ = 0.025, 0.05, 0.10, 0.15, 0.20, 0.25 and 0.30) in Fig. 7(b). First, slight overestimation can be expected when $C_{ID}$ = 0.025 and 0.30 by mean values (1.006 and 1.018, respectively). On the other hand, a slight underestimation or closed outcome can achieve from the $C_{ID}$ range between 0.05 to 0.20. Once again, this is a reliable level of the difference with NLFEM ($R^2$ = 0.99 or above).*

*In this study, we proposed a generalised shape of the empirical formulation in predicting the ultimate limit state of the plate. Furthermore, its applicability was validated by considering initially deflected plate conditions under longitudinal compression. The general shape of the empirical formulation in Eq. (6.1) consists of four coefficients and suits with the specific conditions considered in this study, i.e., $\boldsymbol{k_1}$ = 0.555, $\boldsymbol{k_2}$ = 1.219, $\boldsymbol{k_3}$ = 0.319 and $\boldsymbol{k_4}$ = -0.06 determined by curve-fitting method shown in Eq. (6.2). The accuracy of the empirical formulation obtained in predicting ULS of the simply supported plate under longitudinal compression is also presented in Figs. 8(a) and (b).*

*As summarised in Table 2, only the limited conditions are considered in this study, which means that other conditions could be further considered in the future. Moreover, it is expected that the general shape of the empirical formulation by the present study may be applicable for other conditions (i.e., different end conditions, loading types, material properties, etc.) by formulating the sub-functions of the four coefficients abovementioned. This can be considered an advantage of the present outcome by comparing it with the previous result by Kim et al. (2018c). Details on the difference between previous and present studies may be found in the Appendix.*

*Table 2: Considered conditions for developing an empirical formulation of the rectangle plate.*

| | | | | Present study | Further study |
|---|---|---|---|---|---|
| Boundary condition | | | Simply supported | √ | |
| | | | Clamped | - | TBC |
| | | | Others | - | TBC |
| Finite element model extent (Model size effects on ULS may be referred to ISSC (2003, 2006, 2009, 2012) reports | | | 1bay-1span | √ | |
| | | | 2bay-1span | - | √ |
| | | | 3bay-1span | - | √ |
| | | | Others | - | |
| Geometry | Hole | | Without | √ | |
| | | | With | - | TBC |
| Damage | As-built or construction | Initial imperfection | Initial deflection | √ | |
| | | | Initial crack | - | TBC |
| | | | Localised dent | - | TBC |
| | | | Others | - | TBC |
| | In-service | Ageing | Corrosion | - | TBC |
| | | | Crack propagation | - | TBC |
| | | Accidental | Dropped object | - | TBC |
| | | | Fire | - | TBC |
| | | | Explosion | - | TBC |
| | | | Collision or Grounding | - | TBC |
| | | | Others | - | TBC |
| Initial deflection shape | | | Buckling | √ | |
| | | | Hungry horse | - | TBC |
| | | | Mountain | - | TBC |
| | | | Spoon | - | TBC |
| | | | Others | - | TBC |
| Loading condition | Static or quasi-static | | Longitudinal compression | √ | |
| | | | Transverse compression | - | TBC |
| | | | Shear | - | TBC |
| | | | Lateral pressure | - | TBC |
| | | | Combined loading | - | TBC |
| | Dynamic or Impact | | Similar to the above | - | TBC |
| Material | Type | | Steel (MS24 and HT 32 only) | √ | |
| | | | Aluminium | - | TBC |
| | | | Others | - | TBC |
| | Stress-strain curve | | Bilinear | √ | |
| | | | Multilinear | - | TBC |
| | | | Others | - | TBC |
| Analysis method | | | Experimental | - | TBC |
| | | | Analytical | - | TBC |
| | | | Numerical: NLFEM by ANSYS | √ | |
| | | | Numerical: Others | - | TBC |

*Note: TBC = to be considered or conducted, MS24 = mild steel with 24kgf of yield strength, HT 32 = high tensile steel with 32kgf, NLFEM = nonlinear finite element method.*

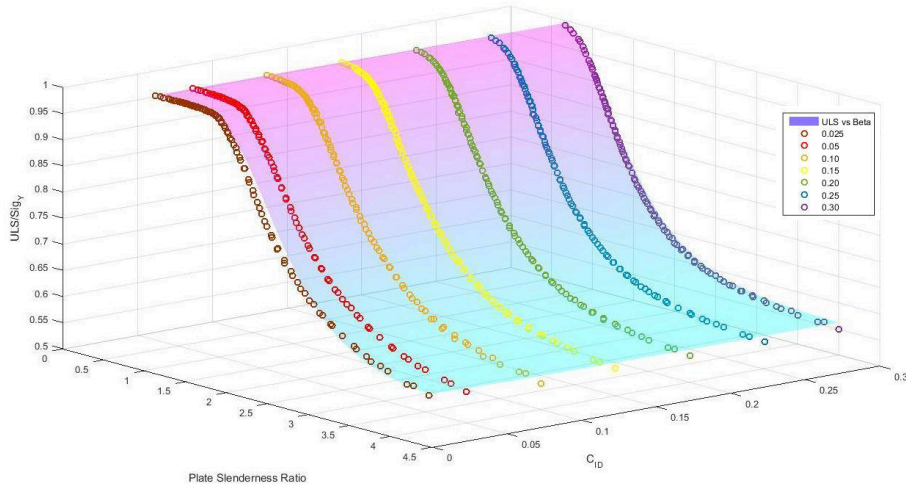


*(a) Proposed empirical formulation (3D view, $R^2$ = 0.996, SSE: 0.07097, RMSE = 0.01005)*

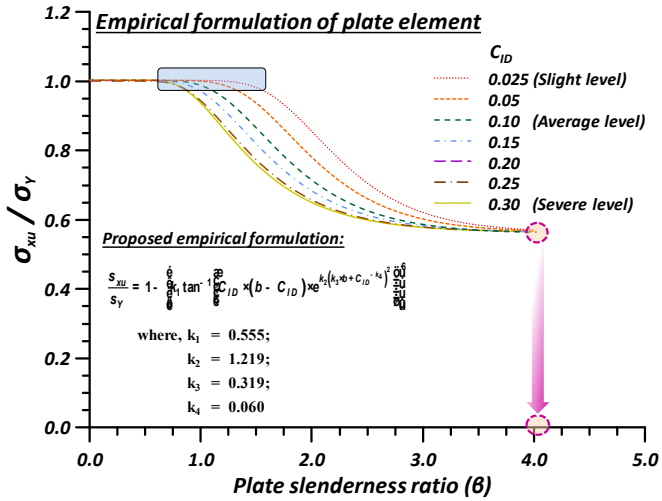


*(b) Proposed empirical formulation (2D view)*

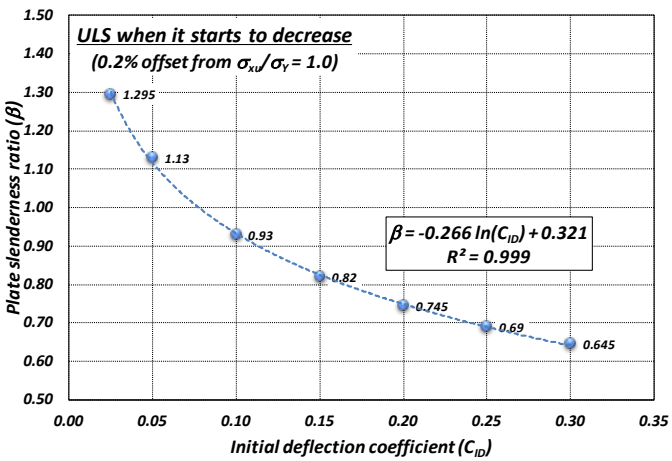


*(c) Decreasing point of ULS*

*Figure 8: Summary of empirical formulation obtained by this study (Continued).*

*From the 3D and 2D curves in Figs. 8(a) and (b), we confirmed that the empirical formulation proposed in this study was well-fitted with NLFEM results ($R^2$ = 0.996 from the 3D fitting graph in Fig. 8). Furthermore, the statistical analysis results such as mean and COV values in Fig. 7(b) may support structural designers to understand its applicability and accuracy when predicting the ultimate compressive strength of the initially deflected plate for the design and safety assessment.*

*We also reconfirm that the ratio between ultimate compressive strength and material yield strength (= $s_{xu}/s_Y$ ) no longer maintains 1.0 as the plate slenderness ratio increases, as shown in Fig. 8(b). It means that ULS starts to decrease when the plate slenderness ratio reaches a specific value. Furthermore, this behaviour is affected by the amount of initial deflection highlighted by the shaded box in Fig. 8(b). With regards to this, we assumed that ULS is decreasing when $s_{xu}/s_Y$ = 0.998 condition satisfied, which is 0.2% offset from $s_{xu}/s_Y$ = 1.0. Based on this assumption, we plotted the relationship between plate slenderness ratio and initial deflection coefficient (= the amount of initial deflection) in Fig. 8(c). For the study purpose, the following trend is also obtained by the curve-fitting method.*

$$b = -\ 0.266 \ln(C_{ID}) + 0.321 \qquad (R^2 = 0.999) \tag{8}$$

*Moreover, we observed that the ratio between ultimate compressive strength and material yield strength (= $s_{xu}/s_Y$ ) tends to crossover when the plate slenderness ratio reaches around 4.0-4.2, as highlighted in Fig. 8(b). From our analysis in the discussion section, ULS is constant when $b$ is less than certain values in Eq. (8). At the same time, ULS tends to crossover when the $b$ values are around 4.0-4.2. From this, it can be concluded that the initial deflection effect is negligible when the plate slenderness ratio is small or very large. It can be understood that a 4.0-4.2 range represents an extremely thin plate from the definition of plate slenderness ratio ( $b = (b/t) \times \sqrt{(s_Y / E)}$ ), which does not recommend in the shipbuilding industry. In addition, we aware that ship structures could be considered moderately thin-walled structures, but the meaning here might not be the same.*

*From the discussion above, we can conclude that the effect of initial deflection amount on ULS is negligible if the plate slenderness ratio is too small (* $\boldsymbol{b}$ £ $-0.266\ln(C_{ID})+0.321$*). Apart from the level of initial deflection, ULS tends to crossover when* $\boldsymbol{b}$ *is getting too much thinner (* $\boldsymbol{b}$ *= 4.0~4.2). This is obtained from the adopted conditions illustrated in Table 2 and could be depending on the condition assumed.*

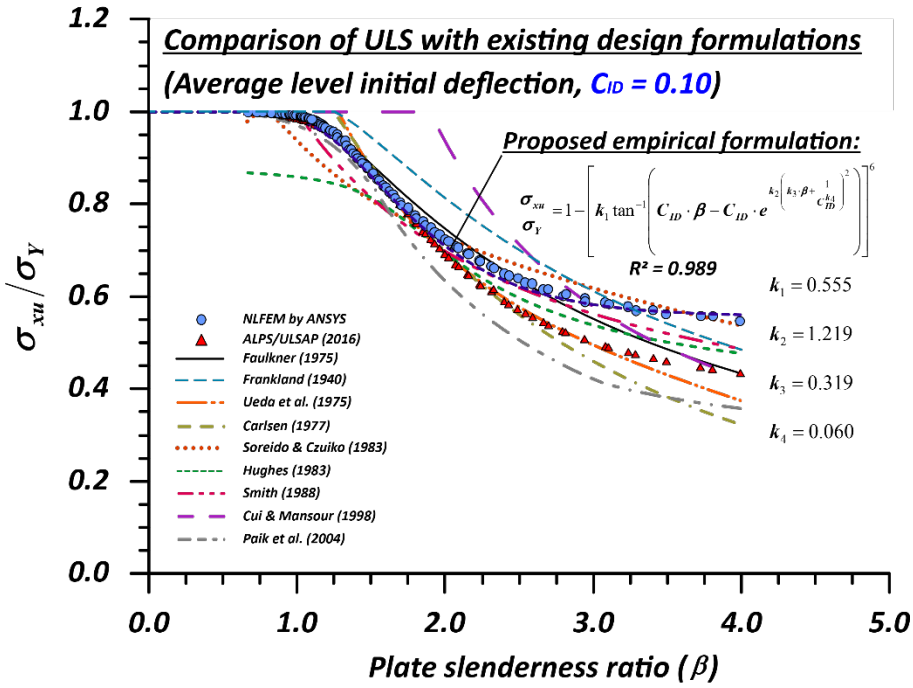


*Figure 9: Comparison of ultimate strength of plate in longitudinal compression with other formulations*

*Lastly, we compared the empirical formulation proposed by this study with existing empirical formulations (Carlsen, 1977; Cui and Mansour, 1998; Faulkner, 1977; Hughes, 1983; Paik et al., 2004; Smith et al., 1988; Soreide and Czujko, 1983; Ueda et al., 1975) shown in Table 3, and semi-analytical solution (ALPS/ULSAP, 2016) shown in Fig. 9. It should be aware that some of the empirical formulations enable us to take into account the effect of initial deflection, but there are more than others. Therefore, the average level of initial deflection (* $C_{ID} = 0.1$*) is only considered for the comparison in Fig. 9.*

*Table 3: Example of the existing empirical formulas in predicting the ultimate strength of the plate.*

| | |
|---|---|
| *Faulkner (1975)* | *Simply supported condition:* $\frac{\sigma_{xu}}{\sigma_Y} = \begin{cases} 1.0 & \beta < 1.0 \\ 2.0/\beta - 1.0/\beta^2 & \beta \geq 1.0 \end{cases}$ |
| *Frankland (1940)* | $\frac{\sigma_{xu}}{\sigma_Y} = \begin{cases} 1.0 & \beta < 1.25 \\ \frac{2.25}{\beta} - \frac{1.25}{\beta^2} & \beta \geq 1.25 \end{cases}$ |
| *Ueda et al. (1975)* | $\frac{\sigma_{xu}}{\sigma_Y} = \frac{1.338\omega_o^{\ 2} + 4.380\omega_o + 2.647}{\beta + 6.130\omega_o + 0.720} - 0.271\omega_o - 0.088$ <br> $\omega_o = \frac{A_{om}}{t};\ A_{om} = C_{ID}\beta^2 t\,.$ |
| *Carlsen (1977)* | $\frac{\sigma_{xu}}{\sigma_Y} = \left(\frac{2.1}{\beta} - \frac{0.9}{\beta^2}\right)\left(1 - \frac{0.75\omega_0}{\beta}\right)(1-\eta);\ \omega_o = \frac{A_{om}}{t};\ A_{om} = C_{ID}\beta^2 t;\ \eta = \frac{-\sigma_{rc}}{\sigma_Y}.$ <br> $\sigma_{rc} = \text{compressive residual stress (as negative value)}$ |
| *Soreide and Czujko (1983)* | $\frac{\sigma_{xu}}{\sigma_Y} = 1.42\left[1 - 2.19\left(\frac{\omega_0}{b/t}\right)^{0.129}\left(\frac{1.26}{\beta} - \frac{1.43}{\beta^2} + \frac{0.55}{\beta^3}\right)\right]\left(\frac{2.74}{\beta} - \frac{2.56}{\beta^2} + \frac{0.92}{\beta^3}\right)$ <br> $\omega_o = A_{om}/t;\ A_{om} = C_{ID}\beta^2 t\,.$ |
| *Hughes (1983)* | $\frac{\sigma_{xu}}{\sigma_Y} = \frac{1}{4}\left(1.6 + \xi - \sqrt{\xi^2 - \frac{10.4}{\beta^2}}\right);\ \xi = 1 + \frac{2.75}{\beta^2}$ |
| *Smith et al. (1988)* | $\frac{\sigma_{xu}}{\sigma_Y} = 0.23 + \frac{1.16}{\beta} - \frac{0.48}{\beta^2} + \frac{0.09}{\beta^3}$ |
| *Cui and Mansor (1998)* | $\frac{\sigma_{xu}}{\sigma_Y} = \begin{cases} 1.0 & \beta \leq 1.9 \\ 0.08 + 1.09/\beta + 1.26/\beta^2 & \beta > 1.9 \end{cases}$ |
| *Paik et al. (2004)* | $\frac{\sigma_{xu}}{\sigma_Y} = \begin{cases} -0.032\beta^4 + 0.002\beta^2 + 1.0 & \beta \leq 1.5 \\ 1.274/\beta & 1.5 < \beta \leq 3.0 \\ 1.248/\beta^2 + 0.283 & \beta > 3.0 \end{cases}$ |

*Once again, we should also recognise that each formulation has developed not the exactly same condition so that it is challenging to compare directly and discuss accuracy here. The current FE results can be considered ideal by adopting buckling mode shape. However, the plate can be deflected by several shapes, such as hungry horse, mountain, spoon, sinusoidal and others. This may affect the ULS behaviour when the plate gets slender (beta > 1.9). In addition, welding-induced residual stress may also affect the ULS behaviour of the plate. In this study, we*

*have not considered the residual stress effect. The above matters may cause the difference of each empirical formula.*

*Nevertheless, plotted results may provide particular insight into the research purpose. In brief, most empirical formulas show good agreement with the FE analysis results when the plate is thick (= plate slenderness ratio ≤ 1.9). The empirical formulation proposed in this study showed good agreement with NLFEM conducted based on assumed condition adopted in this study summarised in Table 2. As summarised in Appendix, one of the strengths of the formulation proposed in this study is the extensibility to take other conditions into account by formulating sub-coefficients. It may be further investigated in the future.*

# 5 Conclusions

*This study investigated the ultimate strength behaviour of initially deflected plates used in ships and offshore construction subjected to longitudinal compression caused by vertical bending. In total, seven hundred plate scenarios were considered for the detailed parametric study by covering the broad range of plate's geometric and material properties adopted in ships and offshore industries. In the case of initial deflection, various level of the deflections such as slight ($C_{ID}$ = 0.025), average ($C_{ID}$ = 0.10), and severe ($C_{ID}$ = 0.30) was considered by assuming buckling shape. Furthermore, other levels of initial deflection, i.e., ($C_{ID}$ = 0.05, 0.15, 0.20, and 0.25) are also adopted for the research purpose. Besides, the general shape of the empirical formulation considered a user-friendly solution is suggested to predict the ultimate compressive strength of the initially deflected plate, which may be usefully applied for the design of the plate element. The main outcome obtained in this study can be summarised as follows.*

- *The general shape of the empirical formulation in predicting the ultimate strength of the plate is proposed in Eq. (7.1).*

- *An empirical formulation in predicting ULS of initially deflected and simply supported edged plate under longitudinal compression is developed based on general shape by determining four coefficients shown in Eq. (7.2).*
- *The statistical analysis was conducted to investigate the effect of the level of initial deflection.*
- *The effect of initial deflection on ULS is investigated as plate slenderness ratio increased shown in Figs. 8(b) and (c).*
- *The results of ULS by NLFEM, semi-analytical method (ALPS/ULSAP, 2016), and direct calculation method by empirical formulations are plotted to compare in Figure 9.*
- *It should be clearly stated that the proposed empirical formulation in Eq. (7.2) is based on the assumed condition in Table 2, and a different set of coefficients could be determined by considering other conditions to be investigated in the future.*

*The effect of the extra high strength steel may also be further investigated in the future, as highlighted in Section 2.1. In addition, only the single kind of buckling half-wave number (= 5.0) is considered in this study so that the other values may also be considered to improve the proposed empirical formula in the future.*

*Lastly, we believe that the general shape of the empirical formulation in Eq. (7.1) may support developing the various conditions summarised in Table 2. Its applicability can be extended soon by performing additional parametric studies summarised in Table 2. Besides, the empirical formulation proposed in Eq. (7.2) may help design the plate element, which is a local structural component. The application study, i.e., an empirical formula in predicting ULS of the plate under combined axial compression and lateral pressure, can also be found in Part 2 (Kim et al., 2022).*

# Acknowledgements

*This work was supported by the New Faculty Startup Fund from Seoul National University and the Brain Pool program funded by the Ministry of Science and ICT through the National Research Foundation of Korea (2021H1D3A2A02094658).*

# References

ALPS/ULSAP, 2016. A computer program for ultimate limit state assessment of plates and stiffened panels. Advanced Technology Center, DRS C3 Systems, Parsippany, NJ, USA.
Ao, L., Wu, H., Wang, D.-y., Wu, W.-g., 2020. Evaluation on the residual ultimate strength of stiffened plates with central dent under longitudinal thrust. Ocean Engineering 202, 107167.
Carlsen, C.A., 1977. Simplified collapse analysis of stiffened plates. Norwegian Maritime Research 5 (4), 20-36.
Cui, W., Mansour, A.E., 1998. Effects of welding distortions and residual stresses on the ultimate strength of long rectangular plates under uniaxial compression. Marine Structures 11 (6), 251-269.
Doan, V.T., Liu, B., Garbatov, Y., Wu, W., Guedes Soares, C., 2020. Strength assessment of aluminium and steel stiffened panels with openings on longitudinal girders. Ocean Engineering 200, 107047.
Dwight, J.B., Moxham, K.E., 1969. Welded Steel Plates in Compression. The Structural Engineering 47 (2), 49-66.
Faulkner, D., 1975. A Review of Effective Plating for Use in the Analysis of Stiffened Plating in Bending and Compression. Journal of Ship research 19 (1), 1-17.
Faulkner, D., 1977. Compression Tests on Welded Eccentrically Stiffened Plate Panels Crosby Lockwood Publishers, London, UK.
Frankland, J.M., 1940. The strength of ship plating under edge compression. EMM report, US.
Georgiadis, D., Samuelides, M., 2019. A methodology for the reassessment of hull-girder ultimate strength of a VLCC tanker based on corrosion model updating. Ships and Offshore Structures 14 (sup1), 270-280.
Gerard, G., 1957. Handbook of structural stability part IV: failure of plates and composite elements. New York University, New York, Washington DC, USA.
Guedes Soares, C., 1988. Design equation for the compressive strength of unstiffened plate elements with initial imperfections. Journal of Constructional Steel Research 9 (4), 287-310.
Hughes, O.F., 1983. Ship structural design: a rationally-based, computer-aided, optimization approach. Wiley-Interscience, New York, NY, USA.
IACS, 2006a. Common Structural Rules for Bulk Carriers. International Association of Classification Societies, London, UK.
IACS, 2006b. Common Structural Rules for Double Hull Oil Tankers. International Association of Classification Societies, London, UK.
IACS, 2020. Common Structural Rules for Bulk Carriers and Oil Tankers. International Association of Classification Societies, London, UK (Available from: http://www.iacs.org.uk/publications/common-structural-rules/csr-for-bulk-carriers-and-oil-tankers).
ISSC, 2003. Ultimate Strength (Committee III.1), The 15th International Ship and Offshore Structures Congress (ISSC 2003), 11-15 August, San Diego, USA.
ISSC, 2006. Ultimate Strength (Committee III.1), The 16th International Ship and Offshore Structures Congress (ISSC 2006), 20-25 August, Southampton, UK.
ISSC, 2009. Ultimate Strength (Committee III.1), The 17th International Ship and Offshore Structures Congress (ISSC 2009), 16-21 August, Seoul, Korea.
ISSC, 2012. Ultimate Strength (Committee III.1), The 18th International Ship and Offshore Structures Congress (ISSC 2012), 9-13 September, Rostock, Germany.
ISSC, 2015. Ultimate Strength (Committee III.1), The 19th International Ship and Offshore Structures Congress (ISSC 2015), 7-10 September, Cascais, Portugal.
ISSC, 2018. Ultimate Strength (Committee III.1), The 20th International Ship and Offshore Structures Congress (ISSC 2018), 9-13 September, Liege, Belgium & Amsterdam, The Netherlands.
Jagite, G., Bigot, F., Derbanne, Q., Malenica, Š., Le Sourne, H., Lauzon, J.d., Cartraud, P., 2019. Numerical investigation on dynamic ultimate strength of stiffened panels considering real loading scenarios. Ships and Offshore Structures 14 (sup1), 374-386.
Jiang, X., Guedes Soares, C., 2012. A closed form formula to predict the ultimate capacity of pitted mild steel plate under biaxial compression. Thin-Walled Structures 59, 27-34.
Khedmati, M.R., Zareei, M.R., Rigo, P., 2010. Empirical formulations for estimation of ultimate strength of continuous stiffened aluminium plates under combined in-plane compression and lateral pressure. Thin-Walled Structures 48 (3), 274-289.
Kim, D.K., Danasakaran, K., Li, S., Cho, N.-K., 2022. An empirical formula to access ultimate strength of initially

deflected plate: Part 2 = Combined axial compression and lateral pressure. Applied Ocean Research, Under review.
Kim, D.K., Incecik, A., Choi, H.S., Wong, E.W.C., Yu, S.Y., Park, K.S., 2018a. A simplified method to predict fatigue damage of offshore riser subjected to vortex-induced vibration by adopting current index concept. Ocean Engineering 157, 401-411.
Kim, D.K., Kim, H.B., Park, D.H., Mohd, H.M., Paik, J.K., 2020a. A practical diagram to determine the residual longitudinal strength of grounded ship in Northern Sea Route. Ships and Offshore Structures 15 (7), 683-700.
Kim, D.K., Lim, H.L., Cho, N.-K., 2020b. An advanced technique to predict time-dependent corrosion damage of onshore, offshore, nearshore and ship structures: Part II = Application to the ship's ballast tank. International Journal of Naval Architecture and Ocean Engineering 12, 645-656.
Kim, D.K., Lim, H.L., Kim, M.S., Hwang, O.J., Park, K.S., 2017. An empirical formulation for predicting the ultimate strength of stiffened panels subjected to longitudinal compression. Ocean Engineering 140, 270-280.
Kim, D.K., Lim, H.L., Yu, S.Y., 2018b. A technical review on ultimate strength prediction of stiffened panels in axial compression. Ocean Engineering 170, 392-406.
Kim, D.K., Lim, H.L., Yu, S.Y., 2019a. Ultimate strength prediction of T-bar stiffened panel under longitudinal compression by data processing: A refined empirical formulation. Ocean Engineering 192, 106522.
Kim, D.K., Park, D.K., Kim, J.H., Kim, S.J., Kim, B.J., Seo, J.K., Paik, J.K., 2012a. Effect of corrosion on the ultimate strength of double hull oil tankers- Part I: stiffened panels. Structural Engineering and Mechanics 42 (4), 507-530.
Kim, D.K., Park, D.K., Park, D.H., Kim, H.B., Kim, B.J., Seo, J.K., Paik, J.K., 2012b. Effect of corrosion on the ultimate strength of double hull oil tankers-Part II: hull girders. Structural Engineering and Mechanics 42 (4), 531-549.
Kim, D.K., Pedersen, P.T., Paik, J.K., Kim, H.B., Zhang, X., Kim, M.S., 2013. Safety guidelines of ultimate hull girder strength for grounded container ships. Safety science 59, 46-54.
Kim, D.K., Poh, B.Y., Lee, J.R., Paik, J.K., 2018c. Ultimate strength of initially deflected plate under longitudinal compression: Part I = An advanced empirical formulation. Structural Engineering and Mechanics 68 (2), 247-259.
Kim, D.K., Wong, E.W.C., Cho, N.-K., 2020c. An advanced technique to predict time-dependent corrosion damage of onshore, offshore, nearshore and ship structures: Part I = generalisation. International Journal of Naval Architecture and Ocean Engineering 12, 657-666.
Kim, D.K., Wong, E.W.C., Lee, E.B., Yu, S.Y., Kim, Y.T., 2019b. A method for the empirical formulation of current profile. Ships and Offshore Structures 14 (2), 176-192.
Kim, D.K., Yu, S.Y., Lim, H.L., Cho, N.-K., 2020d. Ultimate compressive strength of stiffened panel: An empirical formulation for flat-bar type. Journal of Marine Science and Engineering 8 (8), 605.
Kong, X., Yang, Y., Gan, J., Yuan, T., Ao, L., Wu, W., 2020. Experimental and numerical investigation on the detailed buckling process of similar stiffened panels subjected to in-plane compressive load. Thin-Walled Structures 148, 106620.
Lee, D.H., Kim, S.J., Lee, M.S., Paik, J.K., 2019. Ultimate limit state based design versus allowable working stress based design for box girder crane structures. Thin-Walled Structures 134, 491-507.
Lee, D.H., Paik, J.K., 2020. Ultimate strength characteristics of as-built ultra-large containership hull structures under combined vertical bending and torsion. Ships and Offshore Structures, 1-18.
Li, S., Benson, S.D., 2019. A re-evaluation of the hull girder shakedown limit states. Ships and Offshore Structures 14 (sup1), 239-250.
Li, S., Hu, Z., Benson, S., 2020. Progressive collapse analysis of ship hull girders subjected to extreme cyclic bending. Marine Structures 73, 102803.
Li, S., Kim, D.K., Benson, S., 2021. A probabilistic approach to assess the computational uncertainty of ultimate strength of hull girders. Reliability Engineering & System Safety 213, 107688.
Lin, Y.-T., 1985. Ship longitudinal strength modelling. Ph.D. Dissertation, Department of Naval Architecture and Ocean Engineering, University of Glasgow, Scotland, UK.
Mohd, M.H., Kim, D.K., Kim, D.W., Paik, J.K., 2014. A time-variant corrosion wastage model for subsea gas pipelines. Ships and Offshore Structures 9 (2), 161-176.
Ozdemir, M., Ergin, A., Yanagihara, D., Tanaka, S., Yao, T., 2018. A new method to estimate ultimate strength of stiffened panels under longitudinal thrust based on analytical formulas. Marine Structures 59, 510-535.
Paik, J.K., 2007. Empirical formulations for predicting the ultimate compressive strength of welded aluminum stiffened panels. Thin-Walled Structures 45 (2), 171-184.
Paik, J.K., 2008. Some recent advances in the concepts of plate-effectiveness evaluation. Thin-Walled Structures 46 (7), 1035-1046.

Paik, J.K., 2018. Ultimate limit state analysis and design of plated structures (2nd Ed.). John Wiley & Sons, Chichester, UK.
Paik, J.K., Kim, B.J., Seo, J.K., 2008. Methods for ultimate limit state assessment of ships and ship-shaped offshore structures: Part I—Unstiffened plates. Ocean Engineering 35 (2), 261-270.
Paik, J.K., Kim, D.K., Kim, M.S., 2009. Ultimate strength performance of Suezmax tanker structures: pre-CSR versus CSR designs. International Journal of Maritime Engineering 151 (Part A2), 39-58.
Paik, J.K., Kim, D.K., Lee, H., Shim, Y.L., 2012a. A Method for Analyzing Elastic Large Deflection Behavior of Perfect and Imperfect Plates With Partially Rotation-Restrained Edges. Journal of Offshore Mechanics and Arctic Engineering 134 (2), 021603.
Paik, J.K., Kim, D.K., Park, D.H., Kim, H.B., Kim, M.S., 2012b. A new method for assessing the safety of ships damaged by grounding. International Journal of Maritime Engineering 154 (Part A1), 1-20.
Paik, J.K., Seo, J.K., 2009. Nonlinear finite element method models for ultimate strength analysis of steel stiffened-plate structures under combined biaxial compression and lateral pressure actions—Part I: Plate elements. Thin-Walled Structures 47 (8), 1008-1017.
Paik, J.K., Thayamballi, A.K., 1997. An Empirical Formulation For Predicting the Ultimate Compressive Strength of Stiffened Panels, The 7th International Offshore and Polar Engineering Conference (ISOPE 1997), 25-30 May, Honolulu, Hawaii, USA, pp. ISOPE-I-97-444.
Paik, J.K., Thayamballi, A.K., 2007. Ship-shaped offshore installations: design, building, and operation. Cambridge University Press, Cambridge, UK.
Paik, J.K., Thayamballi, A.K., Lee, J.M., 2004. Effect of initial deflection shape on the ultimate strength behavior of welded steel plates under biaxial compressive loads. Journal of Ship research 48 (1), 45-60.
Pei, Z., Gao, C., Fu, J., Takami, T., Iijima, K., Fujikubo, M., Tanaka, Y., Yao, T., 2010a. Development of ISUM Shear Plate Element And Its Application to Progressive Collapse Analysis of Plates Under Combined Loading, The 20th International Offshore and Polar Engineering Conference (ISOPE 2010). International Society of Offshore and Polar Engineers, Beijing, China, pp. 773-780.
Pei, Z., Ji, Y., Nakamaru, K., Tanaka, S., Okazawa, S., Fujikubo, M., Yao, T., 2010b. Development of Isoparametric ISUM Plate Element, The 20th International Offshore and Polar Engineering Conference (ISOPE 2010). International Society of Offshore and Polar Engineers, Beijing, China, pp. 781-788.
Sadovský, Z., Teixeira, A.P., Guedes Soares, C., 2005. Degradation of the compressive strength of rectangular plates due to initial deflection. Thin-Walled Structures 43 (1), 65-82.
Saeidifar, M., Sadeghi, S., Saviz, M., 2010. Analytical solution for the buckling of rectangular plates under uni-axial compression with variable thickness and elasticity modulus in the y-direction. Proceedings of the Institution of Mechanical Engineers, Part C: Journal of Mechanical Engineering Science 224 (1), 33-41.
Shi, G.-j., Gao, D.-w., 2020. Ultimate strength of U-type stiffened panels for hatch covers used in ship cargo holds. Ships and Offshore Structures, 1-12.
Smith, C.S., Davidson, P.C., Chapman, J.C., Dowling, P.J., 1988. Strength and stiffness of ships'plating under in-plane compression and tension. Royal Institution of Naval Architects Transactions 130, 277-296.
Soreide, T.H., Czujko, J., 1983. Load carrying capacities of plates under combined lateral load and axial/biaxial compression, The 2nd International Symposium on Practical Design in Shipbuilding (PRADS 1983), 17-22 October, Tokyo and Seoul, Japan and Korea.
Tanaka, S., Yanagihara, D., Yasuoka, A., Harada, M., Okazawa, S., Fujikubo, M., Yao, T., 2014. Evaluation of ultimate strength of stiffened panels under longitudinal thrust. Marine Structures 36, 21-50.
Tatsumi, A., Fujikubo, M., 2020. Ultimate strength of container ships subjected to combined hogging moment and bottom local loads part 1: Nonlinear finite element analysis. Marine Structures 69, 102683.
Tatsumi, A., Htoo Ko, H.H., Fujikubo, M., 2020. Ultimate strength of container ships subjected to combined hogging moment and bottom local loads, Part 2: An extension of Smith's method. Marine Structures 71, 102738.
Teixeira, A.P., Ivanov, L.D., Guedes Soares, C., 2013. Assessment of characteristic values of the ultimate strength of corroded steel plates with initial imperfections. Engineering Structures 56, 517-527.
Timoshenko, S.P., 1936. Theory of elastic stability. McGraw-Hill New York, NY, USA.
Ueda, Y., Yao, T., 1985. The influence of complex initial deflection modes on the behaviour and ultimate strength of rectangular plates in compression. Journal of Constructional Steel Research 5 (4), 265-302.
Ueda, Y., Yasukawa, W., Yao, T., Ikegami, H., Ominami, R., 1975. Ultimate strength of square plates subjected to compression (1st Report). Journal of the Society of Naval Architects of Japan 1975 (137), 210-221.
Underwood, J.M., Sobey, A.J., Blake, J.I.R., Shenoi, R.A., 2012. Ultimate collapse strength assessment of damaged steel-plated structures. Engineering Structures 38, 1-10.

von Kármán, T., 1924. Die mittragende breite (The effective width), Beiträge zur Technischen Mechanik und Technischen Physik (in German). Springer, pp. 114-127.
Winter, G., 1940. Stress Distribution in and Equivalent Width of Flanges of Wide, Thin-Wall Steel Beams, National Advisory Committee for Aeronautics (NACA) Cornell University, Washington DC, USA.
Wong, E.W.C., Kim, D.K., 2018. A simplified method to predict fatigue damage of TTR subjected to short-term VIV using artificial neural network. Advances in Engineering Software 126, 100-109.
Youssef, S.A.M., Faisal, M., Seo, J.K., Kim, B.J., Ha, Y.C., Kim, D.K., Paik, J.K., Cheng, F., Kim, M.S., 2016. Assessing the risk of ship hull collapse due to collision. Ships and Offshore Structures 11 (4), 335-350.
Zhang, J., Shi, X.H., Guedes Soares, C., Liu, J., 2020. Ultimate strength of stiffened panels with a crack and pits under uni-axial longitudinal compression. Ships and Offshore Structures, 1-20.
Zhang, S., 2016. A review and study on ultimate strength of steel plates and stiffened panels in axial compression. Ships and Offshore Structures 11 (1), 81-91.
Zhang, S., Khan, I., 2009. Buckling and ultimate capability of plates and stiffened panels in axial compression. Marine Structures 22 (4), 791-808.

# [Appendix A] Probability density functions (PDFs)

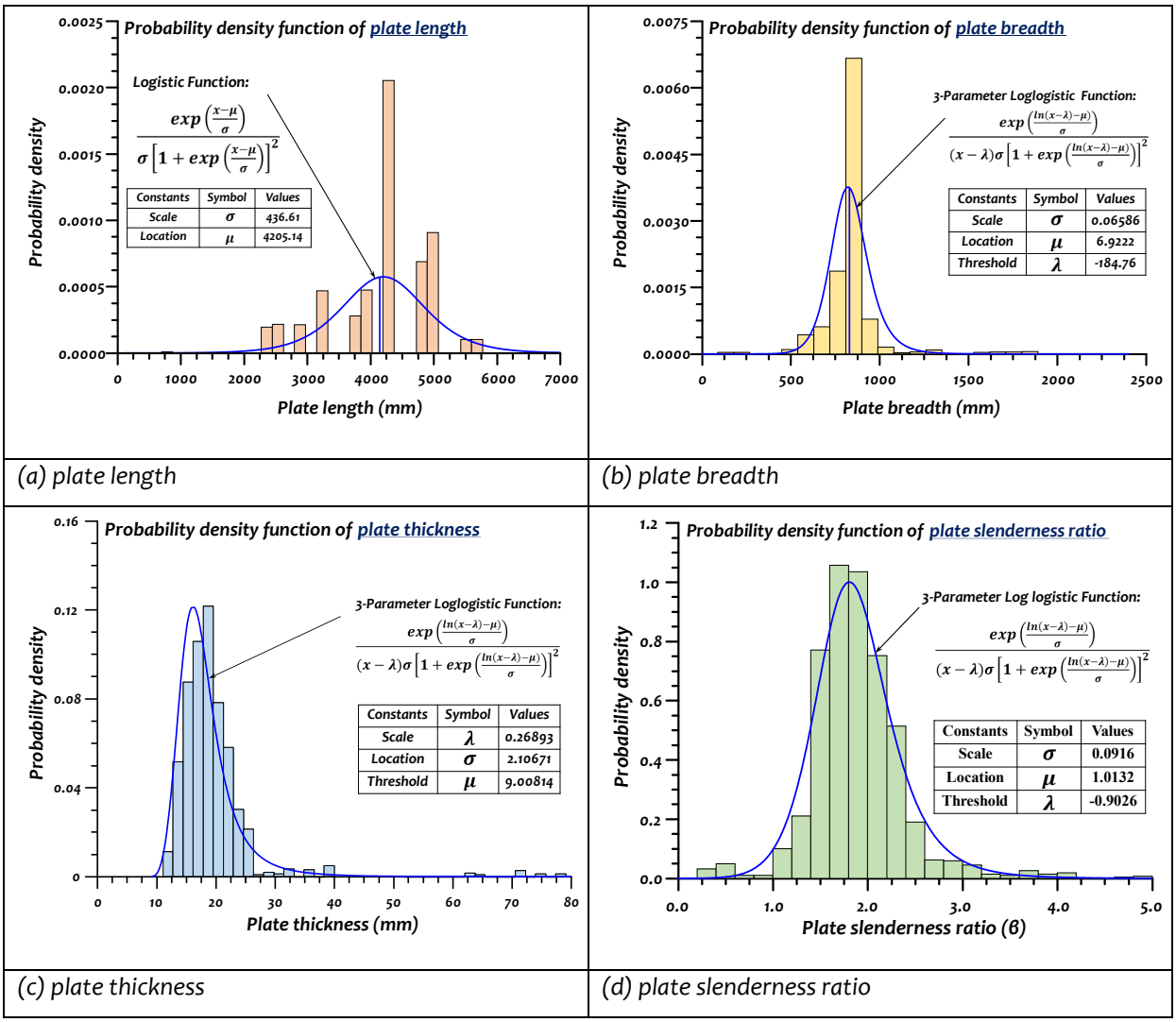


(a) plate length (b) plate breadth

(c) plate thickness (d) plate slenderness ratio

*Figure A.1 Investigated distribution of the probability density of the selected plate from commercial ships (Kim et al. 2018a).*

# [Appendix B] Use of the empirical formuluas

*In this section, we briefly introduce the empirical formulation by Kim et al. (2018c) in predicting the ultimate strength of an initially deflected plate subjected to longitudinal compression. The advantages and disadvantages are also summarised based on the comparison with the present study outcome. The empirical formulation (Kim et al., 2018c) is basically formulated as a function of plate slenderness ratio and four coefficients, as shown in Eq. (A.1).*

$$\frac{\sigma_{xu}}{\sigma_Y} = 1 - \exp\left( \frac{c_1}{\beta} + \frac{c_2}{\beta^2} + \frac{c_3}{\beta^3} + c_4 \right) \tag{A.1}$$

*Where,* $\sigma_{xu}$ *= ultimate strength of plate in longitudinal compression,* $\sigma_Y$ *= material yield strength,* $\beta$ *= plate slenderness ratio (=* $\frac{b}{t}\sqrt{\frac{\sigma_Y}{E}}$*), and* $c_1 - c_4$ *= initial deflection coefficients summarised in Table A.1.*

*Table A.1 Summary of initial deflection coefficients.*

| $C_{ID}$ | $c_1$ | $c_2$ | $c_3$ | $c_4$ |
|---|---|---|---|---|
| 0.025 | -10.749 | 31.246 | -37.009 | 0.48 |
| 0.05 | -2.948 | 8.138 | -13.839 | -0.368 |
| 0.1 | -0.029 | 0.322 | -4.68 | -0.745 |
| 0.15 | 0.735 | -1.554 | -2.172 | -0.859 |
| 0.2 | 1.064 | -2.321 | -1.06 | -0.912 |
| 0.25 | 1.241 | -2.719 | -0.448 | -0.943 |
| 0.3 | 1.349 | -2.956 | -0.068 | -0.963 |

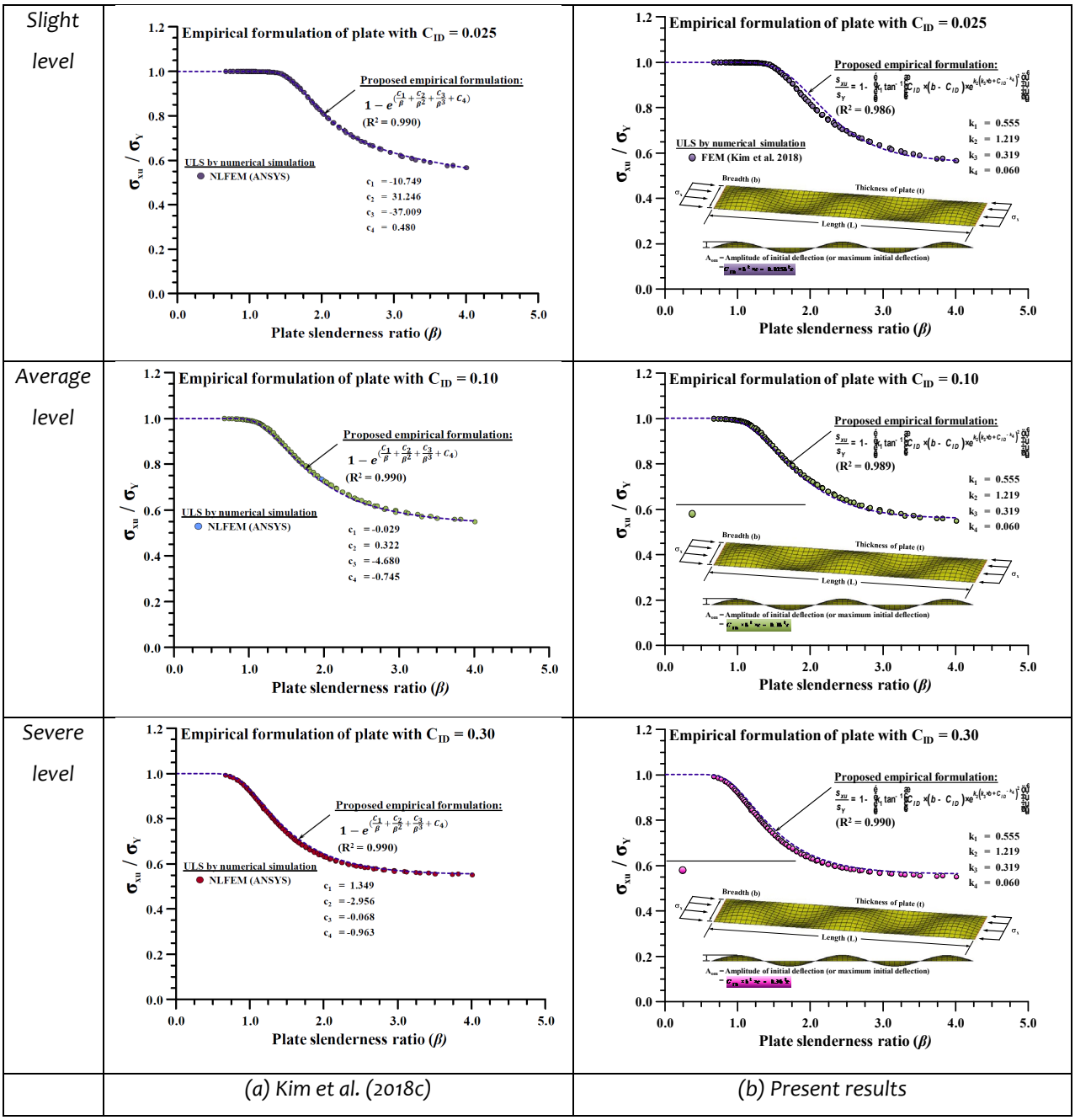


*Figure A1: Typical results of empirical formulas with nonlinear finite element method in predicting ultimate strength of the plate.*

*For the empirical expression (Eq. 7.2) obtained in this study, we found that it lacks accuracy compared to the results of Kim et al. (2018c). This is due to the coefficient effect which constructs the empirical formula. In the case of (Kim et al., 2018c), coefficients vary with the initial deflection of the plate, while the present outcome adopted by the constant coefficients. On the other hand, the proposed empirical expression in this study may be more advantageous*

*to consider the various conditions, as below.*

- ***Loading type***
  - *Axial compression (present study)*
  - *Biaxial compression*
  - *Shear / torsion / etc.*
  - *Lateral pressure*
- *Geometry*
  - *Aspect ratio, etc.*
- *Material properties*
  - *Yield strength, etc.*
- *Initial imperfection*
  - *Initial deflection*
  - *Weld-induced residual stress, etc.*

*This is considered more useful in future studies, considering the combined loads, different material and geometric properties, and many others.*